Role of the aryl hydrocarbon receptor in ultraviolet radiation-induced DNA damage responses of the skin

Inaugural dissertation

for the attainment of the title of doctor
in the Faculty of Mathematics and Natural Sciences
at the Heinrich-Heine-University Duesseldorf

submitted by

Siraz Shaik
from Nellore, India

Duesseldorf, December 2016

From the IUF-Leibniz-Institut für umweltmedizinische Forschung
at the Heinrich-Heine-University Duesseldorf gGmbH

Published by permission of the
Faculty of Mathematics and Natural Sciences at
Heinrich-Heine-University Duesseldorf

Supervisor: Prof. Dr. Jean Krutmann
Co-supervisor: Prof. Dr. Peter Proksch
Oral Exam date - 28-03-2017

Abstract

Exposure to ultraviolet (UV) radiation, particularly its UVB component, is one of the most important risk factors for the development of skin cancer, such as non-melanoma skin cancer (NMSC). When solar light penetrates the skin, high-energy UVB rays are absorbed by the DNA of epidermal keratinocytes (KC) leading to the formation of mutagenic DNA photoproducts, especially cyclobutane pyrimidine dimers (CPDs). To prevent UVB-induced mutagenesis, which may give rise to skin cancer, damaged KC undergo cell cycle arrest and initiate DNA repair. Thus, an increase of DNA repair activity, in most cases, protects the cells from DNA damage and thus counteracts tumorigenesis. The aryl hydrocarbon receptor (AhR) is a ligand-activated transcription factor, which is expressed in KC and is activated in response to UVB-irradiation. UVB-radiation is known to cause DNA-damage-dependent and DNA-damage-independent responses in KC. So far it was well-established that AhR is a crucial mediator of the DNA-damage-independent stress responses, for instance triggering the UVB-mediated induction of pro-inflammatory enzymes. In contrast, if and to which extent AhR signaling affects DNA-damage responses in UVB-exposed KC is quite enigmatic.

Therefore, the aim of the present work was to assess the role of AhR in UVB-irradiated DNA damage responses in KC. For this purpose HaCaT cells, AhR knockdown (HaCaT-shAhR) cells and cutaneous squamous cell carcinoma (SCC) cell-lines have been investigated. Both shRNA-mediated and chemical inhibition of AhR signaling in HaCaT cells resulted in a significantly improved removal of UVB-induced CPDs as shown by southwestern slot blot technique. Further RNAi-based studies targeting the expression of the nucleotide excision repair (NER) enzymes *xeroderma pigmentosum* complementation group A (XPA), XPC, and Cockayne syndrome protein B (CSB) revealed that AhR specifically regulates the global genome repair (GGR) sub-pathway of NER in HaCaT cells. However, instead of rescuing damaged KC from apoptosis, AhR inhibition enhanced UVB-induced apoptosis at later time points upon irradiation. Interestingly the enhanced apoptosis susceptibility of the KC positively correlated with increased DNA double-strand breaks as evidenced by neutral comet assay analyses and gamma-H2AX quantification. Thus, AhR inhibition contributes to both improved CPD removal and increased apoptosis, and thus may be suitable target for chemoprevention of UVB-induced skin malignancies. However, as apoptosis is triggered by DNA double-strand breaks, which may not only initiate cell death but also genomic alterations, this option should be further validated. Since an enhancement of apoptosis susceptibility may be of interest with regards to cancer cell killing, AhR antagonism may foster chemotherapeutic measures. Indeed, genetic,

and chemical AhR inhibition in the two human SCC cell-lines A431 and SCL-1 resulted in elevated apoptotic cell death in response to UVB exposure. Thus, AhR antagonism may present a suitable strategy to improve the therapeutic effect of genotoxic anti-cancer drugs.

These results indicate that the AhR plays a central role in regulating genomic integrity: Whereas AhR inhibits NER and thus fosters skin photocarcinogenesis, it seems to be critical for the proper repair of mitosis-related DNA double-strand breaks.

Table of Contents

List of Figures

List of Tables

List of Abbreviations

6-4PPs	6-4 photoproducts
AhR	aryl hydrocarbon receptor
AhRR	aryl hydrocarbon receptor repressor
AIP	AhR interacting protein
APS	ammoniumpersulphate
ARNT	aryl hydrocarbon nuclear translocator
BaP	benzo(a)pyrene
Bax	bcl-2 associated x protein
BCCs	basal cell carcinomas
bHLH	basic helix loop helix
BSA	bovine serum albumin
CDK	cyclin-dependent kinase
COX2	cyclooxygenase 2
CPDs	cyclobutane pyrimidine dimers
CS	cockyne syndrome
CYP1A1	cytochrome P450 1A1
DEPC	diethylpyrocarbonate
DMBA	dimethyl butylamine
DMEM	Dulbecco's modified eagle medium
DMSO	dimethyl sulfoxide
DNA	deoxyribonucleic acid
DNTPs	deoxynucleotides
DTT	dithiothreitol
EDTA	ethylene diamine tetraacetic acid
EGFR	epidermal growth factor receptor
FACS	fluorescence activated cell sorting
FCS	fetal calf serum
FICZ	6-formylindolo (3,2,-b) carbazole
GGR	global genomic repair
HaCaT	human immortalised keratinocytes
HAHs	halogenated aromatic hydrocarbons
HCl	hydrochloric acid

HSP90	heat shock protein 90
IL-6	interleukin-6
IL-8	interleukin-8
IR	infrared
KC	keratinocytes
MAPK	mitogen-activated protein kinase
MED	minimal erythema dose
MEM	minimum essential medium
MMLV	moloney murine leukemia virus
MNF	3'methoxy-4'nitroflavone
NaCl	sodium chloride
NaOH	sodium hydroxide
NER	nucleotide excision repair
NF	nuclear factor
NMSC	non-melanoma squamous cell carcinoma
NQO1	NAD(P)H dehydrogenase (quinone 1)
PAGE	polyacrylamide gel electrophoresis
PAHs	polycyclic aromatic hydrocarbons
PAS	Per-Arnt-Sim
PBS	phosphate-buffered saline
PCB 126	3,3',4,4',5-pentachlorobiphenyl
PCR	polymerase chain reaction
PER	proteins period
PIC	protease inhibitor cocktail
PMSF	phenylmethylsulfonyl fluoride
pol η	polymerase η
PVDF	polyvinylidene fluoride
RNA	ribonucleic acid
RNAP	RNA polymerase
SCCs	squamous cell carcinomas
SD	standard deviation of the mean
SDS	sodium dodecyl sulfate
SIM	single-minded
siRNA	small interfering ribonucleic acids

SM	skim milk
SWB	south western blot
T4N5	T4 endonuclease V
TAD	transcriptional activation domain
TBS	tris-buffered saline
TCDD	2,3,7,8-tetrachlorodibenzo-p-dioxin
TCR	transcription coupled repair
TEMED	tetraacetylethylenediamine
TLS	trans-lesion DNA synthesis
UV	ultraviolet
WHO	world health organization
XP	xeroderma pigmentosum
XRE	xenobiotic responsive elements

1. Introduction

Exposure to ultraviolet (UV) radiation, particularly its UVB component, is one of the most important risk factors for the development of various skin disorders, such as sunburn, immunosuppression, skin cancer, and premature aging. In the skin, UVB rays are mainly absorbed by the DNA resulting in the formation of highly mutagenic DNA photoproducts (Kulms and Schwarz 2000). Cells with these UVB-induced DNA changes enter cell cycle arrest to eliminate the damage by a specialized repair system. If the damage is too severe and the cell is unable to repair, it initiates programmed cell death. UVB radiation also activates cell-membrane-dependent receptors and subsequent signaling pathways, such as mitogen-activated protein kinases (MAPK) and nuclear factor-kB (NF-kB) (Herrlich et al. 2008, Krutmann et al. 2012). The activation of these molecular pathways can stimulate mitogenic signals and cellular survival, which can contribute to tumor-promoting properties of UVB radiation. In general, a distinction can be made between two limbs of the cellular UVB-stress response: one is directly initiated by DNA damage consisting of the activation of cell-cycle inhibitors, repair, and death pathways, whereas the other one, involving stimulation of mitogenic and anti-apoptotic signal transduction, occurs independently from DNA damage. It has been shown that the aryl hydrocarbon receptor (AhR) plays a significant role in later UVB stress response (Fritsche et al. 2007). UVB-irradiation of keratinocytes leads to the formation of the tryptophan photoproduct 6-formylindolo(3,2,-b)carbazole (FICZ), a high-affinity AhR ligand (Rannug et al. 1987). Upon ligand-binding, the cytosolic AhR dissociates from its co-chaperons and shuttles into the nucleus where it dimerizes with its nuclear partner AhR nuclear translocator (ARNT) and binds to xenobiotic responsive elements (XRE) in the promoter region of target genes (e.g., encoding cytochrome P450 (CYP) 1A1) to induce their transcription. Furthermore, ligand-bound AhR also sends signals to cell membrane, resulting in the activation of the epidermal growth factor receptor (EGFR). This subsequently activates downstream MAPK signaling and results in the transcriptional induction of other genes (e.g., coding for cyclooxygenase-2, COX2). Since an increased expression of CYP activity can lead to the formation of reactive oxygen species (Puntarulo and Cederbaum 1998) and moreover COX2 is involved in UV-induced inflammatory responses and carcinogenesis (Pentland et al. 1999), it was postulated that the AhR plays a critical role in the development of UV-induced skin cancer (Agostinis et al. 2007). It has been demonstrated that transient inhibition of AhR prevents UVB-induced adverse effects in the skin (Agostinis et al. 2007, Haarmann-Stemmann et al. 2012, Krutmann et al. 2012, Frauenstein et al. 2013). However, the contribution of the AhR to the

DNA damage-dependent UVB stress responses, in particular, photo-carcinogenesis, remains to be elucidated.

1.2. The Skin

1.2.1. Structure and function of the skin

The skin is the largest organ in the human body and protects the body and internal organs by forming a covering layer to the outside world. The surface of the skin covers 1.5 to 2 m^2. The most important function of the skin is to form the first line of defense against dangerous external chemical, biological and physical agents. Moreover, it prevents the body from drying, regulates heat and water balance, allows us to sense stimuli, and is involved in vitamin D synthesis. The skin receives the most solar radiations from the sun. Solar radiations are important as they provide warm conditions and maintain circadian rhythms for proper functioning and survival of various living creatures on the earth's surface. Solar radiations also play an important role in the physiology and pathophysiology of the skin. In general, the human skin is divided into three different layers: the epidermis (outer skin), dermis (corium) and hypodermis (subcutaneous adipose tissue) (Figure 1).

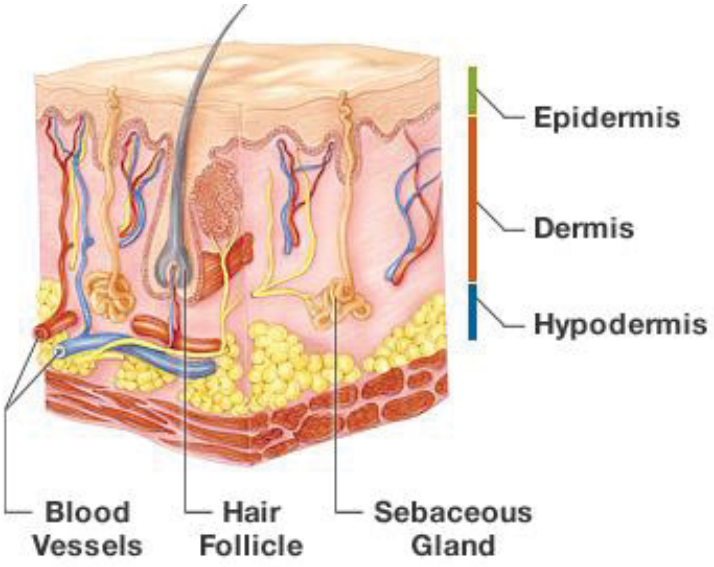

Figure 1 Structure of the skin.
Skin structure is with different layers namely epidermis, dermis, and hypodermis. Blood vessels, hair follicle, and sebaceous gland (Hoffman 2014).

1.2.2. Epidermis

The epidermis is the outermost layer of the skin. It is a stratified epithelium that consists of five different layers of keratinocytes (KC), including the basal layer (stratum basale), the spinous

layer (stratum spinosum), the granular layer (stratum granulosum), the translucent layer (stratum lucidum), and the cornified layer (stratum corneum). Different types of cells are present in the epidermis. The predominant cell type is KC: they make around 90% of the skin and are responsible for making keratin. Other cell types in the epidermis are melanocytes, Langerhans cells, Merkel cells, and lymphocytes; some of these cells are resident cells while some are recruited upon specific conditions. Melanocytes produce the pigment melanin; this is transferred to the adjacent KC to protect the nucleus of the epidermal cell against UV irradiation (Miyamura et al. 2007). Langerhans cells are present in all layers of the epidermis, but most prominently in the spinous layer. Langerhans cells serve as the immunological barriers of the epidermis (Kubo et al. 2009). Merkel cells in the basal epidermal layer are in contact with somatosensory nerve fibers and function as mechanoreceptors (Moll et al. 2005). Lymphocytes are components of the adaptive immune system; they protect the skin against invading microorganisms and are recruited upon specific immune responses (Baroni et al. 2012). Mast cells and macrophages are also present; they help in the immune functions of the cells (Hoffman 2014) (Bukowsky 2010, Jain 2012).

1.2.3. Dermis

The dermis, present beneath the epidermis, is connected to it via the basement membrane. The dermis comprises 70–80% of collagen and 4% of elastic tissue; these tissues provide elasticity and tensile strength. It includes the eccrine, apocrine, and sebaceous glands. Eccrine glands regulate body temperature through evaporative heat loss. Apocrine glands are important in secretion functions, such as secreting sweat. Sebaceous glands are important as they secrete sebum. Apart from these glands, the dermis is enriched in hair follicles, blood vessels, nerve endings, and lymphatic vessels. It also contains fibroblasts, mast cells, and macrophages. Mast cells are rich in histamine and heparin; they play an important role in protecting hypersensitive skin by inflammation processes. Macrophages serve as phagocytes and engulf the exogenous organisms or proteins; products formed after the degradation of melanin or fats are important to maintain the physiological structure of the skin. Beneath the dermis is the hypodermis. The hypodermis contains fat cells and forms the connection between skin, muscle, and bone. The hypodermis supplies the blood vessels and nerve fibers to the upper layers of the skin (Jain 2012).

1.3. Solar spectrum

The electromagnetic radiation that reaches earth's surface ranges from wavelength 290 – 10^6 nm and is divided into three major bands ultraviolet (UV) radiation (290 – 400 nm), visible light (400-760 nm) and infrared (IR) radiation (760 – 10^6 nm). The UV spectrum is further divided into UVA (320nm – 400nm), and UVB (280 – 320 nm) and UVC (100-280nm) (Figure 2). The spectrum and dose of radiation reaching human skin are mainly dependent on the composition of the ozone layer, clouds, the altitude of the sun to earth's surface and ground reflections (Schroeder et al. 2008b). However, 54% of the total solar radiation reaching human skin is IR as compared to 7% UV radiation (Schroeder et al. 2008a, Schroeder et al. 2009).

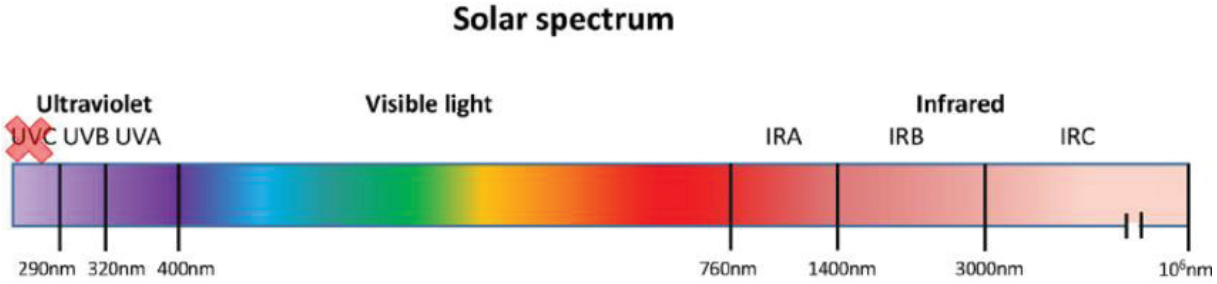

Figure 2 The solar spectrum.
Scheme representing the wavelength range of ultraviolet radiation reaching earth's surface from 290-400 nm, visible light from 400 – 760 mm, and infrared radiation from 760 – 10^6 nm. Further, infrared is divided into IRA, IRB, and IRC. (Barolet et al. 2016).

1.3.1. UV radiation and its effects on the skin

Solar radiation plays an important role in the physiology and pathophysiology of the skin. It is important for vitamin D synthesis, maintenance of the circadian rhythm, and regulation of body temperature. However, an overdose of UV radiation can lead to acute and chronic pathophysiological effects. The acute effects of UVB radiation include sunburn, immunosuppression, and pigmentation (Bowden 2004). Chronic exposure to UVB radiation may lead to skin cancer and premature aging of the skin (Sklar et al. 2013). UVB radiation is known to initiate and promote skin cancer and is thus defined as a complete carcinogen (WHO 2012). When the skin is exposed to sun, UVB rays are primarily absorbed by the epidermis. This results in the formation of two major genotoxic lesions in DNA (Figure 3)-cyclobutane pyrimidine dimers (CPDs) and 6-4 photoproducts (6-4 PPs) (Brash 1988). The incidence of CPDs is five times higher than that of 6-4 PPs, while 6-4 PPs are repaired more rapidly than CPDs (Meador et al. 2000). T4 endonuclease V (T4N5) is an enzyme of bacterial origin that repairs CPDs. Topical application of T4N5 liposomes was found to initiate improved CPD removal in the human and murine skin and was associated with a reduced occurrence of UVB-

induced tumors in a photo-carcinogenesis study in mice. These observations indicate that CPDs play a more important role in skin carcinogenesis than 6-4 PPs do (Yarosh et al. 1992).

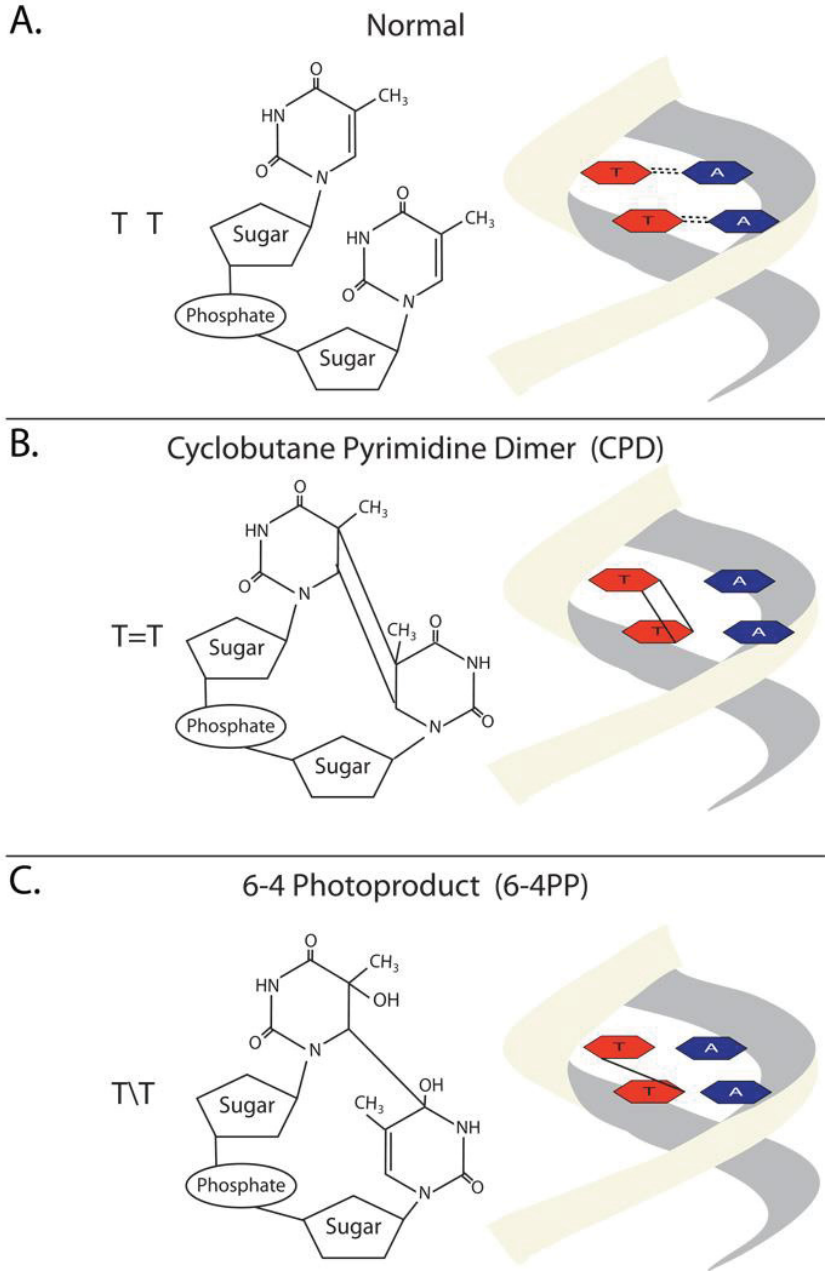

Figure 3 CPDs and 6-4PP generated after UVB irradiation.
DNA molecule with two normal thymidine residues (A). DNA molecule with cyclobutane pyrimidine dimer (B). DNA molecule with 6-4 photoproduct (C). (Maverakis et al. 2010).

If the DNA damage is not repaired before replication, mutations may be introduced into the DNA. If these DNA lesions affect oncogenes or tumor suppressor genes, skin cancer may develop. Thus, the formation of CPDs is one of the most important steps in the development of skin cancer (Brash and Ponten 1998). Also, it has been described that there is a causal link between CPDs and UVB-mediated immunosuppression, which enables the unhampered proliferation of mutant cells and thus promotes the growth and progression of the tumor

(Berneburg and Krutmann 2000). Various repair mechanisms exist to prevent mutagenesis. Upon DNA damage detection, the cell initiates cell-cycle arrest and DNA repair. If the extent of damage is too severe, programmed cell death (apoptosis) is initiated.

1.4. Skin Cancer

According to the World Health Organization (WHO), two to three million cases of non-melanoma and 132,000 cases of melanoma skin cancer occur globally every year. Apart from very rare cutaneous malignancies, non-melanoma skin cancer comprises basal cell carcinomas (BCCs) and squamous cell carcinomas (SCCs). These cancers are seldom mortal; however, surgical treatment is usually painful and leaves scars (WHO). Skin cancer foundation statistics state that one in every five individuals in the US will develop skin cancer in their lifetime (Robinson 2005). A major risk factor for skin cancer development is chronic exposure to UV radiation. The cellular DNA absorbs UV-radiation and generates CPDs and 6-4PPs. In general, the cytosine base in DNA is quite stable; however, the cytosine base in CPD is quite unstable and easily deaminates to an uracil base. When these cytosine bases are synergistically changed to uracil bases, they represent the UV-specific mutation by CPDs. When these CPDs reside on the template strand during replication, they stall the replication. Cells try to excise these lesions through specialized repair mechanisms, such as nucleotide excision repair (NER). Failure to repair these lesions before the replication fork leads to the stall and collapse of the fork at the damaged site, which in turn leads to double-strand breaks and eventually to cell death. To avoid such unfavorable conditions, cells use several mechanisms. One such mechanism is translesion DNA synthesis (TLS). In TLS, DNA polymerase attempts to overcome replication blocks by restarting the DNA synthesis that was stopped at the damaged bases on the template strand. TLS-mediated DNA synthesis is highly error-prone and introduces mutations into the genome. However, DNA polymerase (polη) is specifically functional in CPDs and efficiently suppresses UV irradiation-induced mutations by employing error-free TLS opposite to CPDs. Patients with *xeroderma pigmentosum* (XP-V) who are deficient in polη show high sensitivity to photocarcinogenesis in the regions exposed to solar radiation. Thus, polη induces error-free TLS activity to suppress CPD-mediated mutagenesis. However, it could also unintentionally induce C → T and CC → TT mutations in the uracil-containing CPDs produced by deamination (Ikehata and Ono 2011). Frequent targets of tumor initiators include the activation of oncogenic pathways, such as the epidermal growth factor receptor (EGFR) family and downstream signal transducers, and the mutational inactivation of apoptotic pathways, such as tumor suppressor pathways (e.g., p53), and DNA repair mechanisms (e.g., NER). Tumour promotion describes

the cellular and molecular events leading to the establishment and growth of initiated cells through clonal expansion, development of apoptosis resistance, generation of autocrine growth signals, and other processes (Rakoff-Nahoum 2006). In contrast to mutagenesis, tumor promotion is considered to be a reversible process (Ghantous et al. 2012). Well-characterized examples of potent tumor promoters are TCDD, phenobarbital, and phorbol ester. Tumour progression is a process of enhanced growth speed of tumor cells and their invasion (metastasis).

1.5. DNA repair

DNA is constantly exposed to a variety of exogenous and endogenous noxae that may lead to DNA damage. In addition to exposure to UV radiation and chemical agents, the process of DNA replication itself may cause spontaneous lesions in the DNA. In mammals, UVB-induced DNA adducts are repaired by the NER (Figure 4). NER also contributes to the repair of other helix-distorting lesions, for instance, those induced by polycyclic aromatic hydrocarbons (PAHs) such as Benzo(a)pyrene (BaP) and cytotoxic drugs, such as cisplatin (Wood 1999).

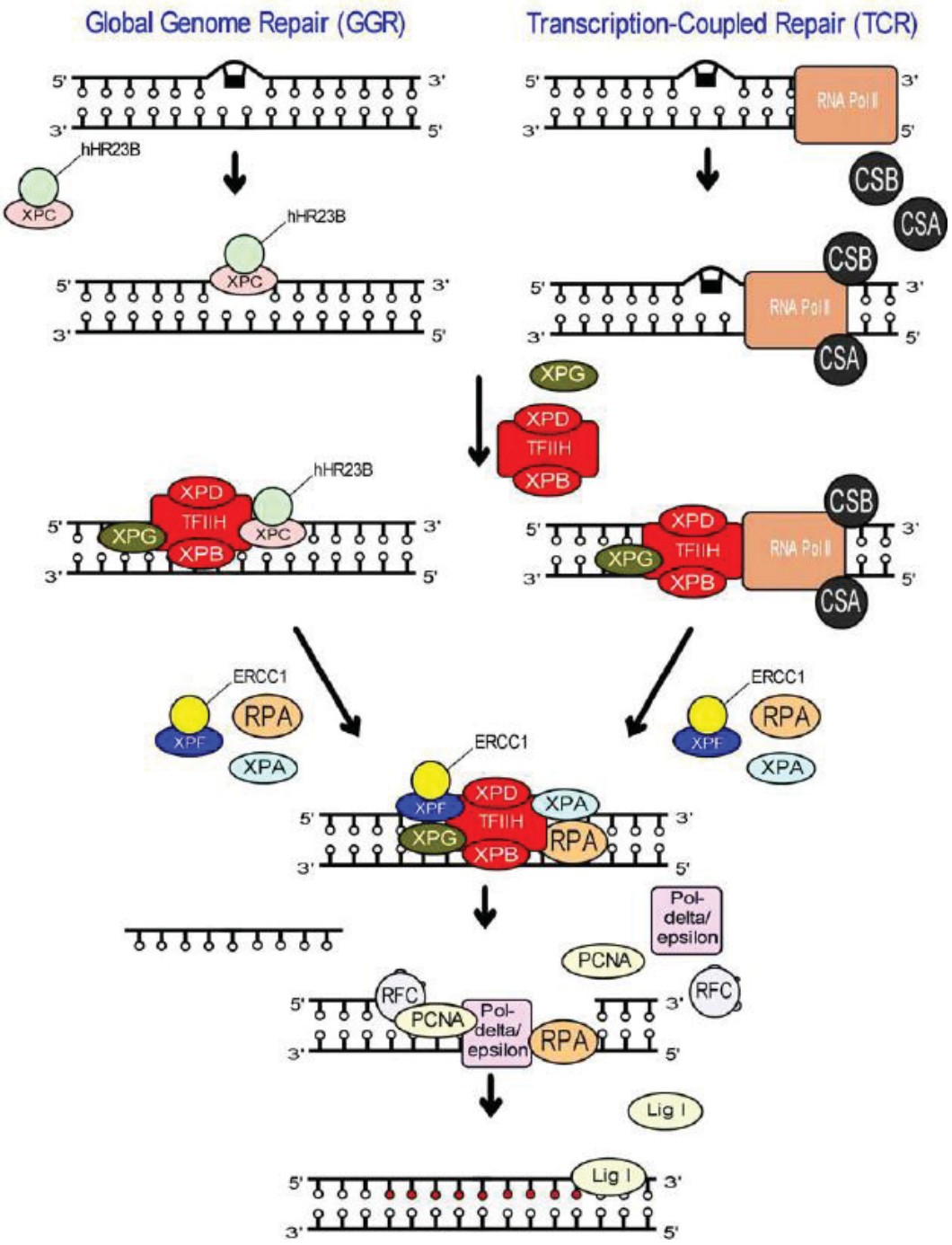

Figure 4 Different steps in nucleotide excision repair (NER).
Four steps in NER are recognition of the DNA damage, unwinding of DNA, excision of damage and gap-filling. (Maverakis et al. 2010).

The process of NER is divided into four steps-recognition of the DNA damage, unwinding of DNA, excision of damage, and gap-filling. Depending on the nature and location of the DNA damage, there are two sub-types of NER-global genomic repair (GGR) and transcription-coupled repair (TCR). As the name suggest, the objective of GGR is to repair damage to the whole genome. In actively transcribed genes, TCR is initiated by stalling an elongated

ribonucleic acid polymerase (RNAP), which stimulates DNA repair five to 10 times faster (Lindahl and Wood 1999). Generally, GGR is a stepwise process that starts with the recognition of the DNA-distortion, probably by XPC-hHR23B protein. XPA is responsible for damage verification and acts downstream of XPC. In the second step, the unwinding of DNA takes place through ATP-dependent helicase activities of XPB and XPD, two subunits of the TFIIH complex (Marteijn et al. 2014). In the third step, DNA is cleaved 5'-upstream and 3'-downstream to excise damage on the dimer by ERCC1 and XPG. After that, the 24-32-base-pair oligonucleotide is released. In the fourth step, the DNA polymerase fills the gap, followed by sealing of the DNA-nick by DNA ligase. In contrast to GGR, the way of damage recognition is different in TCR; it requires RNA polymerase II at the DNA damaged site and Cockayne syndrome (CS) proteins CSA and CSB.

1.6. Aryl hydrocarbon Receptor (AhR)

The AhR is a ligand-activated transcription factor. The AhR, together with its related proteins AhR Nuclear Translocator (ARNT) and AhR Repressor (AhRR), belongs to the family of proteins sharing basic helix loop helix (bHLH) PER-ARNT-SIM (PAS) homology. The structure of the AhR protein is shown in Figure 5. In AhR, the bHLH domain is essential for DNA-binding and protein dimerization (Gu et al. 2000). The PAS domain is located next to the bHLH domain. Initially, the PAS domain was described as a conserved motif in three proteins, the *Drosophila melanogaster* proteins period (PER), single-minded (SIM), and human ARNT protein (Citri et al. 1987, Nambu et al. 1991). The PAS domain is important for heterodimerization with ARNT as well as with other chaperones, such as heat shock protein 90 (HSP90). The PAS domain includes two subdomains: PAS-A and PAS-B. The PAS-B domain of AhR harbors a ligand-binding pocket (Gu et al. 2000). The glutamine (Q)-rich transactivation domain (TAD) represents a transcriptional activation domain. This interacts with several transcriptional co-activators and is important for the activation of target genes (Rowlands et al. 1996).

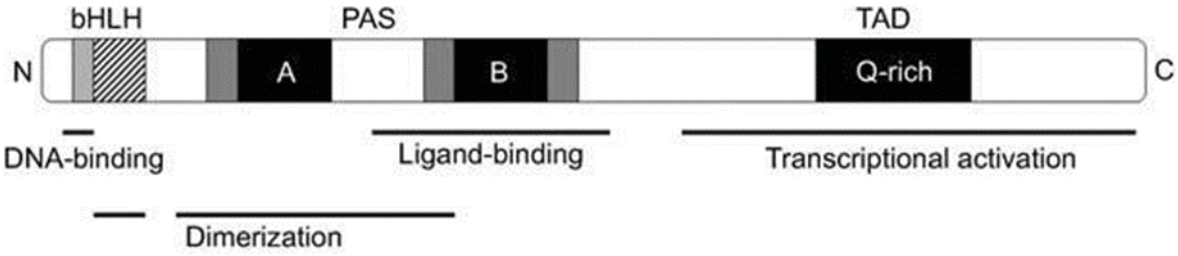

Figure 5 Structure of Aryl hydrocarbon Receptor (AhR).
bHLH, basic-helix-loop-helix domain; PAS, PER-ARNT-SIM domain; TAD, a transcriptional activation domain, N,amino-terminal; C,carboxy-terminal DNA-binding domain, Ligand-binding domain, Transcriptional activation domain, and Dimerization domain. (Abel and Haarmann-Stemmann 2010).

AhR activation is achieved by the ligands binding to the PAS-B domain of AhR (Abel and Haarmann-Stemmann 2010). AhR-binding ligands can be divided into two types: anthropogenic chemicals, including environmental contaminants as well as drugs, and natural compounds from microorganisms, plants, animals, or humans themselves (endogenously synthesized). An overview of relevant ligands of the AhR is given in Table 1.

Table 1 Categories of AhR-binding chemicals and their representative compounds (Abel and Haarmann-Stemmann 2010).

Ligand group	**Compound**
Halogenated aromatic Hydrocarbons	3,3',4,4',5-pentachlorobiphenyl (PCB 126)
	2,3,7,8-Tetrachlorodibenzo-*P*-dioxin
	2,3,7,8-Tetrachlorodibenzofuran
Polycyclic aromatic hydrocarbons	Benzo[a]pyrene
	7,12-Dimethyl-benz[a]anthracene
	3-Methylcholanthrene
Indole derivatives	6-Formylindolo[3,2,-b]carbazole
	2-(1'H-Indole-3'-carbonyl)-thiazole-4-
	Carboxylic acid methyl ester
Alkaloids	Annomontine
	Berberine
	Rutaecarpine
Polyphenols	Curcumin
	Quercetin
	Resveratrol

Pharmaceuticals	Diclofenac
	Omeprazole
	Sulindac

Ligands can activate (agonist) or inhibit (antagonist) the transcriptional activity of AhR. Most high-affinity AhR ligands are synthetic chemicals, including halogenated aromatic hydrocarbons (HAHs) and PAHs (Denison and Nagy 2003). There are other synthetic compounds that bind to AhR with low to medium affinities, such as omeprazole and pesticides, such as carbaryl and thiabendazole (Quattrochi and Tukey 1993, Delescluse et al. 2001). The tryptophan derivatives FICZ and 2-(1'H-Indole-3'-carbonyl)-thiazole-4-Carboxylic acid methyl ester are endogenous ligands that bind to the AhR protein with high affinity (Song et al. 2002). Naturally occurring ligands mainly come from plant ingredients such as polyphenols and alkaloids. Some plant polyphenols that are known to inhibit AhR activity are quercetin, kaempferol (Ciolino et al. 1999), luteoline (Bothe et al. 2010), resveratrol (Ciolino and Yeh 1999), and curcumin (Ciolino et al. 1998), while 3'-methoxy-4'-nitroflavone (MNF) is a synthetic AhR antagonist (Lu et al. 1995).

In the absence of a ligand, AhR is bound to a multiprotein complex in the cytosol. It consists of two HSP90 molecules (Denis et al. 1988), co-chaperone p23 (Kazlauskas et al. 1999), and the immunophilin-like AhR-interacting protein (AIP) (Ma and Whitlock 1997). In addition, the association of tyrosine kinase c-Src with the multiprotein complex is discussed (Enan and Matsumura 1996). If a ligand binds to the receptor, a conformational change occurs and the AhR protein disassociates from the multiprotein complex (Figure 6). The activated AhR translocates to the nucleus and binds to its nuclear partner ARNT (Probst et al. 1993). The heterodimer AhR-ARNT recognizes specific DNA motifs known as xenobiotic responsive elements (XRE) in the promoter region of AhR target genes and induces their transcription.

The probably best characterized target gene of AhR is *CYP1A1*, which codes for the cytochrome P450 1A1 (Vanden Heuvel et al. 1993). The dissociation of AhR from its multiprotein complex after ligand binding also leads to the release of soluble tyrosine kinase c-Src, which may lead to the activation of the non-canonical AhR pathway. Upon stimulation, c-Src may translocate to the cell membrane and activate the EGFR (Enan and Matsumura 1996) and downstream MAPK signal transduction. This results in the transcriptional induction of another set of genes,

e.g., cyclooxygenase 2 (COX2). In addition to the classical AhR target genes, which encode phase 1 enzymes, such as CYP1A1, CYP1B1, and COX2 and phase II enzymes, such as NAD(P)H dehydrogenase (quinone 1) (NQO1) and glutathione S-transferase, the AhR also regulates the expression of some other genes involved in cell proliferation, cell differentiation, cell growth, and apoptosis. For example, an AhR-dependent increased expression of pro-apoptotic Bax (bcl-2-associated x protein) and increased apoptosis in oocytes after PAH treatment have been reported (Matikainen et al. 2001).

Furthermore, the interaction of the AhR with subunits of the NF-kB transcription factor family is described. NF-kB is a transcription factor found in all cell types and tissues. The activation of NF-kB is of great importance in regulating immune responses, such as inflammation (Tian 2009). AhR binding to the NF-kB subunit RelB leads to ARNT-independent transcriptional regulation of interleukin-8 (IL-8) (Vogel et al. 2007, Vogel et al. 2011). Interaction of the AhR with the RelA subunit leads to modulation of interleukin-6 (IL-6) (Chen et al. 2012). The AhR also interferes with other signaling pathways by interacting with proteins such as retinoblastoma protein-1 (Puntarulo and Cederbaum 1998) and the estrogen receptor-α (Bock and Kohle 2009).

1.6.1. Activation of AhR upon UVB irradiation

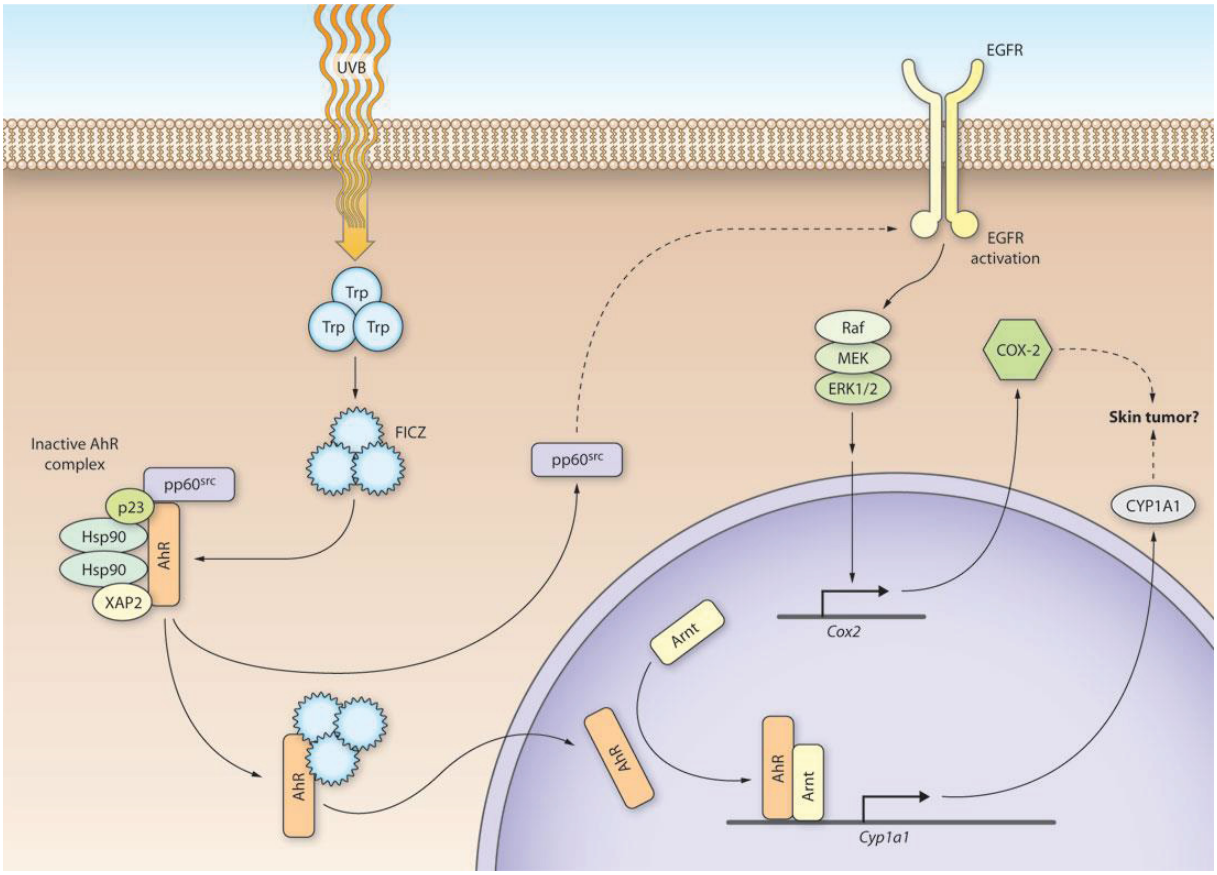

Figure 6 Activation of AhR signaling pathway upon UVB irradiation.
AhR is localized in the cytosol in its inactive form, UVB absorption by tryptophan (Trp) converts it into FICZ, which is AhR ligand and activates it. The activated AhR shuttles into the nucleus and binds with its nuclear partner ARNT to induce the transcriptional activation of target gene *CYP1A1*. Through another unknown mechanism Src triggers the activation of EGFR and downstream MAPK pathway which leads to the phosphorzlation of ERK1/2 and results in the increased expression of *COX2*. (Agostinis et al. 2007).

AhR plays an important role in UVB-induced stress responses in KC (Fritsche et al. 2007). It is well-established that UVB irradiation induces CPDs. Apart from this, it has been shown that UVB radiation activates cell-membrane-bound receptors independently from DNA damage (Herrlich et al. 2008). However, the actual mechanism for the activation of cell-membrane-bound proteins was not well known, e.g. for EGFR (Agostinis et al. 2007). Further, it was shown that UVB irradiation results in the increased expression of CYP1A1 and CYP1B1 protein and gene expression levels in the human skin, suggesting there is a UVB-induced formation of an AhR agonist (Katiyar et al. 2000). Rannug et al. have shown that a derivative of L-tryptophan, upon UVB irradiation, activates AhR; later, it came to be known as FICZ (Rannug et al. 1987, Wei et al. 1998, Fritsche et al. 2007). FICZ is considered as the most potent ligand among both exogenous and endogenous AhR ligands (Rannug et al. 1987, Wincent et al. 2009, Farmahin et al. 2014). After UVB irradiation, gene expression for both *CYP1A1* and *COX2* is upregulated

in KC. This suggests that both canonical and non-canonical AhR pathways are activated by UVB (Fritsche et al. 2007). In non-canonical pathways, exposure of cells UVB radiation leads to activation of cell-membrane-mediated receptor EGFR. The mechanism behind the UVB-induced activation of this receptor is largely unknown. This is followed by the activation of downstream MAPK signaling (RAS-RAF-MEK-ERK1/2) and finally, leads to a transcriptional up-regulation of pro-inflammatory *COX-2* genes (Enan and Matsumura 1996, Haarmann-Stemmann et al. 2009).

It is known that treatment of keratinocytes and murine skin with various plant flavonoids, such as naringenin and epigallacatechin-3-gallate, before UVB exposure results in an improved removal of CPDs (Meeran et al. 2006, El-Mahdy et al. 2008). Interestingly, these plant flavonoids have also been identified to antagonize AhR (Palermo et al. 2003, Zhang et al. 2003), This indicates that the modulation of AhR activity may have an impact on CPD clearance.

Aims

UVB-irradiation can elicit DNA damage-dependent and DNA damage-independent responses in keratinocytes. The later one is at least partially mediated by the AhR. There is evidence in the literature that AhR inhibition can affect DNA repair. Therefore, the purpose of this study is, to assess the role of AhR activation in the UVB-induced DNA damage response in KC.

Specifically, the following questions will be addressed:

1. Is AhR involved in CPD clearance of UVB-irradiated HaCaT keratinocytes?
2. What is the role of AhR in nucleotide excision repair?
3. What is the influence of AhR on UVB-induced apoptosis?

2. Materials and Methods

2.1. Cell culture

Five different cell lines listed in (Table 2) were used for the current study. They were cultured in Dulbecco's modified eagle medium (DMEM), minimum essential medium (MEM), antibiotics/antimycotics (A/A 10.000 µg/ml) and fetal calf serum (FCS). Phosphate-buffered saline (PBS) and trypsin were used for washing and trypsinization respectively. All reagents for the cell culture were purchased from Biochrom, Berlin, Germany.

Table 2 Human cell lines used in this project.

Name of cell line	Description	Medium composition
HaCaT	Immortalized human keratinocytes	DMEM, 10% (v/v) FCS, 10 µg/ml A/A
HaCaT-ev	HaCaT cells, stably transfected with pCL1P.THPC (empty vector)	DMEM, 10% (v/v) FCS, 10 µg/ml A/A, 0.54 mg/ml G418
HaCaT- shAhR	HaCaT cells, stably transfected with pCL1P.THPC (sh RNA for AhR vector)	DMEM, 10% (v/v) FCS, 10 µg/ml A/A, 0.54 mg/ml G418
A431	Human squamous cell carcinoma cell line	MEM, 10% (v/v) FCS, 10 µg/ml A/A, 2% non-essential amino acids
SCL-1	Squamous cell carcinoma cell line	DMEM, 10% (v/v) FCS, 10 µg/ml A/A

All cells were grown under standard conditions (5% CO_2 and 37° C). The medium was changed every alternate day. When the cells reached 80% confluency, they were passaged. For passaging cells were washed thoroughly with PBS, shortly incubated with trypsin at 37 ºC for the cells to detach. The new medium was used to rinse the cells from the flask. Cells were seeded in new

flasks or 6 well plates. After seeding the cells were incubated in the plates overnight. The cells were counted with a hemocytometer, the number of cells used for various experiments is listed below in Table 3.

Table 3 Cell numbers for various experiments.

Experiment	Plate format	Cell number
South-western slot blot	6 well plates	3×10^5 cells/well
Western blot	6 well plates	3×10^5 cells/well
qRT-PCR	6 well plates	3×10^5 cells/well
Transfection	6 well plates	1.5×10^5 cells/well
Comet assay	6 well plates	3×10^5 cells/well
FACS analysis	6 well plates	3×10^5 cells/well

The cells were frozen in liquid nitrogen for long term storage. For this purpose, the cells were detached with trypsin from the bottom of cell culture flasks, centrifuged at 300×g for 5 min, suspended with medium containing 10% (v/v) FCS and 10% (v/v) DMSO and transferred into sterile freezing vials. For cryopreservation, the vials were first incubated at -80º C and then stored in liquid nitrogen.

2.2. Cell exposure

2.2.1. UVB irradiation

For UVB irradiation, the cells were seeded in 6 well plates (Table 3). Cells were rinsed with 2 ml of warm PBS buffer. After rinsing, one ml of warm PBS buffer was added to the cells in 6 well plates. UVB irradiation was carried out with a TL20W/12RS lamp (wavelength range: 290-320 nm) and with an emission peak at 310 nm (Philips, Eindhoven, The Netherlands). After irradiation, the PBS buffer was removed, and own culture medium (Table 2) was immediately

added. Sham-irradiated cells were subjected to the identical procedure just without being irradiated to UVB.

2.2.2. Chemical exposure

After UVB irradiation, cells were treated with chemicals (Table 4). Therefore, cells were seeded (Table 3). For the treatment, the particular chemical was diluted. Cells were incubated in appropriate medium, mixed thoroughly and then applied to cells in the tissue culture plates. All the chemicals were dissolved in DMSO, and the concentration of DMSO was kept 0.1% to avoid potential cytotoxicity.

Table 4 Final concentrations of chemicals used.

Chemicals	End concentration	Solvent	Target
3‘-Methoxy-4‘-Nitroflavon (Symrise, Holzminden)	20 µM	DMSO	AhR inhibitor
Roscovitine (Enzo Life Science)	10 µM	DMSO	CDK inhibitor
PD98059 (Sigma – Aldrich)	10 µM	DMSO	MEK inhibitor
Bosutinib (Sigma – Aldrich)	10 µM	DMSO	Src family kinase inhibitor
PD153035 (Sigma – Aldrich)	10 µM	DMSO	EGFR inhibitor
Wortmannin (Sigma – Aldrich)	10 µM	DMSO	PI3K inhibitor

2.3. siRNA interference

The siRNA is also known as short interfering RNA or silencing RNA, which are double stranded RNA molecules consisting of 20-25 base pairs. siRNAs are used to transiently knock down gene expression, as they degrade complementary mRNAs in transfected cells. For siRNA, interference cells were seeded (Table 3). Transient transfection of HaCaT KC with XPA, XPC, CSB, $p27^{KIP1}$ and non-silencing siRNA (Santa Cruz Biotechnology) was done using

INTERFERIN transfection reagent (Polyplus, New York, USA). Briefly, after 24h the efficiency of transfection was analyzed by western blotting, and the cells were used for Southwestern blot analysis.

2.4. Transfection of cells for overexpression experiments

For overexpression experiments, cells were seeded (Table 3). Transient transfection of HaCaT cells with pCMV5p27 (referred to as pp27; addgene; plasmid #14049), pcDNA5-rAhRR (referred to as pAhRR, provided by Y. Inouye, Toho University Japan), and respective empty vectors was performed using JetPIE transfection reagent (peqlab Erlangen, Germany). Twenty-four hours after transfection, efficiency of $p27^{KIP1}$ or AhRR overexpression was assessed by western blot analysis or PCR, respectively.

2.5. Southwestern slot blot analyses

Southwestern slot blot is a semi-quantitative technique used to detect CPDs in DNA. In this method, the denaturated DNA samples are transferred to a positively charged nylon membrane. The CPDs in the DNA bound membrane are detected with the antibody against it.

2.5.1. Isolation and determination of DNA concentration

For southwestern slot blot, the cells were seeded (Table 3) and incubated overnight. The cells were 50% confluent during the treatment. After treatment, the total DNA of HaCaT cells was extracted using Roche High Pure PCR template preparation kit (Roche Diagnostics GmbH Mannheim, Germany) according to the manufacturer's instructions. The DNA quantity and quality were analyzed with a TECAN instrument (Infinite® 200 PRO, Grödig, Austria).

2.5.2. Spotting of DNA on nitrocellulose membrane

For spotting DNA, equal amounts of DNA were diluted in $TE_{10/1}$ - buffer (pH-8). The DNA was denatured in boiling water for 5 min. Then it was cooled down using an ice bath for 5 min. Later the DNA samples were spotted on positively charged nitrocellulose membrane (GE Healthcare) using a slot blot chamber coupled with a vacuum module. The pressure of vacuum was adjusted between 30-40 kPa.

2.5.3. Denaturation of membrane and detection of CPD's

The membrane-bound DNA was denatured for 45 min on Whatman paper soaked with 0.4 N NaOH. After that, the membranes were blocked in 5% (w/v) skim milk in TBS-T at 4° C overnight. Next day the membranes were incubated with HRP linked thymine dimer antibody (Kamiya Biomedical Company, Seattle, WA) in 5% skim milk (SM)/TBS-T for 2h at room temperature. Next, membranes were washed three times for 10 min with TBS-T buffer. Signals were detected using chemiluminescent Western bright ECL substrate (Advansta) followed by autoradiography. Densitometric analysis of the signals was done using AlphaeaseFC software (Alpha Innotech). Reagents used in the southwestern slot blot analyses are listed in Table 5.

Table 5 Reagents used for southwestern slot blot.

$TE_{10/1}$ – buffer	10 mM	Tris-HCl, pH-8
	1 mM	EDTA (ethylene diamine tetraacetic acid)
TBS – T	10 mM	Tris
	150 mM	NaCl
	0.5% (v/v)	Tween (freshly added)
Denaturation buffer	0.4 N	NaOH
SM/TBS-T (SWB)	5% (w/v)	Skim milk in TBS-T buffer for SWB

2.6. RNA analysis

In this study, mRNA level was analyzed by performing qRT-PCRs.

2.6.1. Isolation and determination of concentration of total RNA

For RNA analysis cells were seeded according to (Table 3), incubated overnight. For the qRT-PCR, the total RNA was isolated using peq GOLD total RNA isolation kits (Peq lab Erlangen) according to the manufacturer's instructions. The RNA quantity and quality were determined spectrophotometrically with a Nanodrop 2000c (Nanodrop, Technologies, Wilmington, DE, USA). The ratio of absorbance at 260 nm and 280 nm is used to assess the purity of RNA. A ratio of approximately (2) is accepted as pure for RNA. RNA can be stored at -80 ºC or can be used for subsequent cDNA synthesis.

2.6.2. cDNA synthesis

For cDNA synthesis, the isolated RNA was reverse transcribed into cDNA. For each sample, 500 ng of total RNA was reverse transcribed to cDNA using Moloney Murine Leukemia Virus (MMLV) reverse transcriptase (Promega, Madison, WI, USA) in a total volume of 20 µl. For this 500 ng of total RNA was diluted in 7.75 µl DEPC-water, then 1.25 µl oligo (dt15) primers (Jena Bioscience, Jena, Germany) and one µl deoxynucleotides (dNTPs; 100 mM) (Jena Bioscience, Jena, Germany) were added. Reverse transcription was performed in a Thermo block, Biometra (Göttingen, Germany). Annealing was done for 5 min at 65º C. After that; the reaction mixture was cooled to 4º C before one µl of MMLV reverse transcriptase, and four µl of 5x RT buffer (both from Promega, Madison, WI, USA) were added. The reverse transcription was done at 37° C for 52 min. Finally, the reverse transcriptase was heat-inactivated at 70º C for 10 min. The obtained cDNA was used immediately or stored at -20º C.

2.6.3. Quantitative real-time PCR

For qRT-PCR cDNA was diluted 1:3 using RNAse free water. For each reaction 3 µl of diluted cDNA, 7.5 µl of SYBR green mix, 2.5 µl of 4 µM forward and reverse primers (Table 6) were used. The PCR amplification was performed in a Rotor-gene 6000 Real-Time PCR machine (Qiagen, Hilden, Germany), by hot start at 95°C for 5 min and using the following set up.

Denaturation	94°C	15s	40 cycles
Annealing	56°C	30s	
Elongation	72°C	30s	

Table 6 Primers used for qRT-PCR

Transcript	Forward primer (5' – 3')	Reverse primer (5' - 3')
XPA	TCTGTGATTGCCTTCTTACAACAGA	CCTTGGTATCTTGTCCTCAAATTTG
XPB	GAGGAAGACTTGGCGTTTTCG	CTAAGCATCATTTCCTAAAGCG
XPC	AAGTTCACTCGCCTCGGTTGC	TTCTTTCCTGATTTTAGCCTTTTT
XPD	ACCCAGGATGGTGCCGAAACCAG	ACCATGAGGCCGTAGTCCGTCTTG

CSB	GATGTCGTACATGACGTGAGG	TATGACCAGGACGTGCTG
CYP1A1	AGACACTGATCTGGCTGCAG	GGGAAGGCTCCATCAGCATC
β-Actin	CCCCAGGCACCAGGGCGTGAT	GGTCATCTTCTCGCGGTTGGCCTT GGGGT

For evaluation of the results, Rotor-Gene Q Series Software 1.7 (Qiagen, Hilden, Germany) was used.

2.7. SDS-PAGE and western blot analysis

SDS-PAGE western blot is a semi-quantitative technique used to detect specific proteins from total protein extract. It uses gel electrophoresis to separate native proteins and a reference size ladder to enable detection of the protein size of interest.

2.7.1. Protein extraction

For western blot analysis, cells were seeded (Table 3), incubated overnight and treated when they reach 50% confluency. Total protein was extracted by washing the cells with PBS and then lysed in RIPA buffer (Table 7) supplemented with 2 µl / ml protease inhibitor cocktail (PIC, Calbiochem, La Jolla, CA, USA) and 5 µl / ml phenylmethylsulphonyl fluoride (PMSF, Sigma-Aldrich) for 10 min on ice. Then the cell lysates were transferred to 1.5 ml Eppendorf tubes and centrifuged for 15 min at 4º C (14.000 RPM) to separate cell debris from proteins. The supernatant was stored in new tubes and used for further analysis.

Table 7 Composition of RIPA buffer for protein extraction.

RIPA-buffer:	25 mM	Tris-HCl, pH-7.4
	150 mM	NaCl
	0.1 mM	EDTA, pH-8
	1% (w/v)	Nonidet p-40
	1% (w/v)	Desoxycholate
	0.1% (w/v)	SDS
	0.025% (w/v)	NaN_3

	2 µl/ml	Protease inhibitor cocktail, freshly added
	200 mM	Phenylmethanesulfonyl fluoride (PMSF), freshly added

2.7.2. Determination of protein concentration

The concentration of isolated proteins was determined using DC protein assay (Bio-Rad, Richmond, VA, USA) as per manufacturer's instructions. According to the principle of Lowry, this assay is based on the reaction of protein with an alkaline copper tartrate solution and folin reagent.

The Protein concentration was calculated based on BSA protein standard curve using a TECAN plate reader (Gröding, Austria).

2.7.3. SDS-polyacrylamide gel electrophoresis (SDS – PAGE)

Sodium dodecyl sulfate-polyacrylamide gel electrophoresis (SDS-PAGE) is a method used for the separation of proteins in an electric field based on their molecular size. To obtain the sharp separation of proteins, a two-gel system was used where all proteins are concentrated or packed in one band in a stacking gel, and protein separation takes place according to the molecular size in a resolution gel. For every sample, equal amounts of proteins were diluted in distilled water and supplemented with 4x loading buffer (Table 8). Before loading on the SDS gel, proteins were denatured for 5 min at 95º C. The protein samples were run on the SDS gel using Mini Vertical Dual Plate Electrophoresis Unit Standard apparatus (Roth, Karlsruhe, Germany) for 30 min at 90 V in stacking gel. Subsequently, protein samples were separated on resolution gel for 2.5 h at 120 V based on their molecular weights. The composition of reagents used in SDS-PAGE is listed in (Table 8).

Table 8 Reagents for SDS – PAGE.

4x loading buffer	250 nM	Tris-HCl, pH-8
	20% (w/v)	Glycerol
	5% (w/v)	SDS
	0.001% (w/v)	Bromophenol blue
	100 mM	DTT (dithiothreitol)
	16%	ß – mercaptoethanol, freshly added

SDS-PAGE running buffer	50 mM	Tris
	383 mM	Glycin
	0.1%	SDS
Stacking gel (5%) for 6 ml	3.5 ml	H_2O
	0.6 ml	Acrylamide (40% v/v)
	0.6 ml	1M Tris pH – 6.8
	24 µl	SDS (20% w/v)
	24 µl	APS (ammoniumpersulphate 20% w/v)
	4.8 µl	TEMED (tetramethylethylenediamine)
Resolution gel (10%) for 12 ml	5.6 ml	H_2O
	3 ml	Acrylamide (40% v/v)
	3.12 ml	1.5 M Tris pH-8.8
	60 µl	SDS (20% w/v)
	60 µl	APS (ammoniumpersulphate 20% w/v)
	60 µl	TEMED (tetramethylethylenediamine)

2.7.4. Western blotting

For transferring the separated proteins from gel to polyvinylidene fluoride (PVDF) membrane, tank transfer method from Roth was used as per manufacturer's instructions. Before starting the transfer, PVDF membrane was activated in methanol and the proteins were transferred from the gel to PVDF membrane in an electric field (100 V, 400 mA for 1h). The composition of the transfer buffer is shown in (Table 9).

Table 9 Transfer buffer for western blot analysis.

Transfer buffer	25 mM	Tris
	192 mM	Glycine
	20% (v/v)	Methanol

2.7.5. Immunodetection of proteins

For immunodetection of proteins, the PVDF membranes were sequentially blocked for 30 min at room temperature with 5% skim milk in TBS-T and 5% BSA in TBS-T. After blocking, the

membranes were incubated with diluted primary antibodies overnight at 4° C. The next day primary antibody was removed, and the membranes were washed three times for 10 min each with TBS-T buffer. After that blots were incubated with a corresponding HRP-conjugated secondary antibody for 1h, followed by another washing step as described above. Visualization of proteins was performed by using the chemiluminescent WesternBright ECL substrate (Advansta, Menlo Park, CA) and X-ray films. Densitometry was carried using AlphaeaseFC software (Alpha Innotech, San Leandro, CA). The reagents used were listed in (Table 10).

Table 10 Reagents used for protein detection.

TBS-T buffer	50mM	Tris – HCl (pH-7.4)
	150mM	NaCl
	0.1% (v/v)	Tween 20
SM/TBS-T	5% (w/v)	Skim Milk in TBS-T buffer
BSA/TBS-T	5% (w/v)	BSA (bovine serum albumin) in TBS-T buffer

Table 11 Antibodies and their final concentration used in the western blot analysis.

Antibody	Provider	Final concentration
AhR	EnoGene (#300170)	1:1000 in SM/TBS-T
ARNT	Cell Signaling (#3718)	1:1000 in BSA/TBS-T
XPA	Sigma (#1254)	1:1000 in SM/TBS-T
XPB	Santa Cruz Biotechnology (#271500)	1:1000 in BSA/TBS-T
XPC	Cell Signaling (#12701)	1:1000 in BSA/TBS-T
XPD	Cell Signaling (#11963)	1:1000 in BSA/TBS-T

CSB	Genetex (#104589)	1:1000 in BSA/TBS-T
p-ERK1/2 (Thr202/Tyr204)	Cell Signaling (#9101)	1:1000 in BSA/TBS-T
T-ERK1/2	Cell Signaling (#9102)	1:1000 in BSA/TBS-T
γ H2AX	Cell Signaling (#2577)	1:1000 in BSA/TBS-T
GAPDH	Cell Signaling (#2118)	1:1000 in SM/TBS-T
CHK1	Cell Signaling (#2360)	1:1000 in SM/TBS-T
PARP	Abcam (#32071)	1:1000 in SM/TBS-T
$P27^{KIP1}$	Cell signaling (#3686)	1:1000 in BSA/TBS-T
Anti-Rabbit IgG, HRP linked	Cell signaling (#7074)	1:2500 in BSA/TBS-T
Anti-mouse IgG, HRP linked	GE-Healthcare (#RPN4201)	1:2500 in SM/TBS-T

2.8. Neutral comet assay

For analyses of DNA double strand breaks, neutral comet assay was performed by embedding the cells in low-melting-point agarose followed by cell lysis under neutral conditions, and electrophoresis.

2.8.1. Preparation of agarose coated super frost slides

For the preparation of agarose coated super frost slides, 0.75% (w/v) agarose (Sigma-Aldrich, Steinheim, Germany) solution was prepared in PBS. Super frost slides were pre-coated with this agarose solution by dipping the slides in hot agarose solution. The excess agarose was wiped off from the back of the slides. They were dried at room temperature and stored back in the slide boxes until further use.

2.8.2. Cell preparation for comet analysis

HaCaT cells were seeded in 6 well plates (Table 3), incubated overnight and treated when they were 50% confluent. To prepare the cells for comet analysis, cells were washed twice with PBS

and detached with trypsin 0.05% / EDTA 0.02% (w/v). Trypsinization was stopped by adding roughly 500 µl of DMEM medium. After this procedure, cells were kept on the ice. 20 µl cells (approximately 1000 cells) and 120 µl of 0.5% low melting agarose solution (Sigma-Aldrich, Steinheim, Germany) were pipetted on pre-coated superfrost slides (see 2.6.1) followed by sealing the gel using a cover slip and 5 min incubation on ice for gel solidification.

2.8.3. Lysis and electrophoresis

Further steps were performed under dark conditions, to avoid DNA damage from light. For lysis, the slides were transferred to vertical staining jars containing lysis buffer. The cells were lysed for at least 1h. Alternately cells could be kept in lysis buffer for up to one week at 4º C. After lysis; the slides were washed briefly for three times with distilled water. The slides were then transferred into an electrophoresis tank containing electrophoresis buffer for 20 min followed by 10 min electrophoresis at 26-28 V. The slides were washed for 5 min 3 times with cold neutralization buffer.

2.8.4. Dehydration, staining, and analysis

After electrophoresis, the slides were kept in absolute ethanol for 5 min and then air dried, or they were stored for further analysis at 4º C. For staining 50 µl ethidium bromide (2 µg/ml water) was pipetted on the super frost slide and sealed with a coverslip. For analysis, replicates of 50 cells per treatment were analyzed using a camera connected microscope (Olympus BX60, Tokyo, Japan). In this thesis, the tail moment was used as a parameter to characterize the comet. Tail moment is the product of percentage of tail DNA and tail length. Comet assays 4.0 software was used to analyze the tail moment of comets. Table 12 shows the reagents employed in the comet assay.

Table 12 Reagents used in neutral comet assay.

Lysis buffer (pH-9.5)	2.5 M	NaCl
	100 mM	EDTA
	10 mM	Tris pH-10
	1% (v/v)	Triton X-100 (freshly added)
	10%	DMSO (freshly added)

Electrophoresis buffer (pH-8.5)	300 mM	NaOH
	1 mM	EDTA
Neutralization buffer (pH-7.5)	0.4 M	Tris

2.9. FACS analysis with Annexin V / propidium iodide staining

Using the Annexin V / propidium iodide staining apoptotic, and necrotic cells in the cell population can be measured. Since it was not possible to differentiate between late apoptotic and necrotic cells both apoptotic and necrotic cells were measured. The enzyme Annexin V binds to phosphatidylserine (PS) residues on the cell surface. Normally phosphatidylserine is present inside the cell, but when the cell undergoes apoptosis or cell death, this lipid comes to the cell surface (Bratton et al. 1997). Propidium iodide is an intercalating agent bind to the nucleic acids in the dead cells. For FACS analysis cells were seeded (Table 3). Cells were treated when they are 50% confluent. For harvesting, the cells were washed twice with PBS buffer and trypsinated at 37 ºC for 5 min and were stopped by adding 500 µl of medium containing FCS. Cells were collected in FACS tubes and performed with Annexin V-FITC Apoptosis kit (BioVision, Milpitas, CA) in combination with an FACScalibur (BD Bioscience, Heidelberg, Germany) according to the manufacturer's protocol. Both apoptotic and necrotic cells were measured. The results were analyzed by Flowing Software version 2.5.1 (Perttu Terho, Turku, Finland).

2.10. Statistics

All the results are presented as the mean and standard deviation of the mean (SD). Statistical software Graph Pad Prism (Graph Pad Software, Inc., San Diego, CA, USA) is used to calculate the results and plot the graphs. To calculate the statistical significance in the normally distributed data Student’s t-test is used with significance levels less than 5% ($p < 0.05$) is considered as significant.

3. Results

3.1. AhR represses the clearance of UVB-induced CPDs in KC

CPDs are UVB-induced DNA photoproducts. It is well established that UVB irradiation induces the formation of CPDs in KC (Qin et al. 1994). Therefore, the effects of irradiation on HaCaT were examined using 200 J/m^2 UVB, which is equal to the minimal erythema dose (MED) of fair-skinned individuals (Martínez-Lozano et al. 2002). DNA was sampled at zero, two, four, eight, and 24 hours after irradiation, followed by CPD content measurement. There was no significant decrease in the CPDs up to four hours. After eight hours, there was a significant reduction in CPD content, and after 24 hours, only 10% of the initial CPD content was left (Figure 7). Since no significant CPD clearance was observed up to four hours, this time point was chosen for further mechanistic analyses. There were no detectable CPDs in sham-irradiated controls. Therefore, this will not be shown in the subsequent experiments.

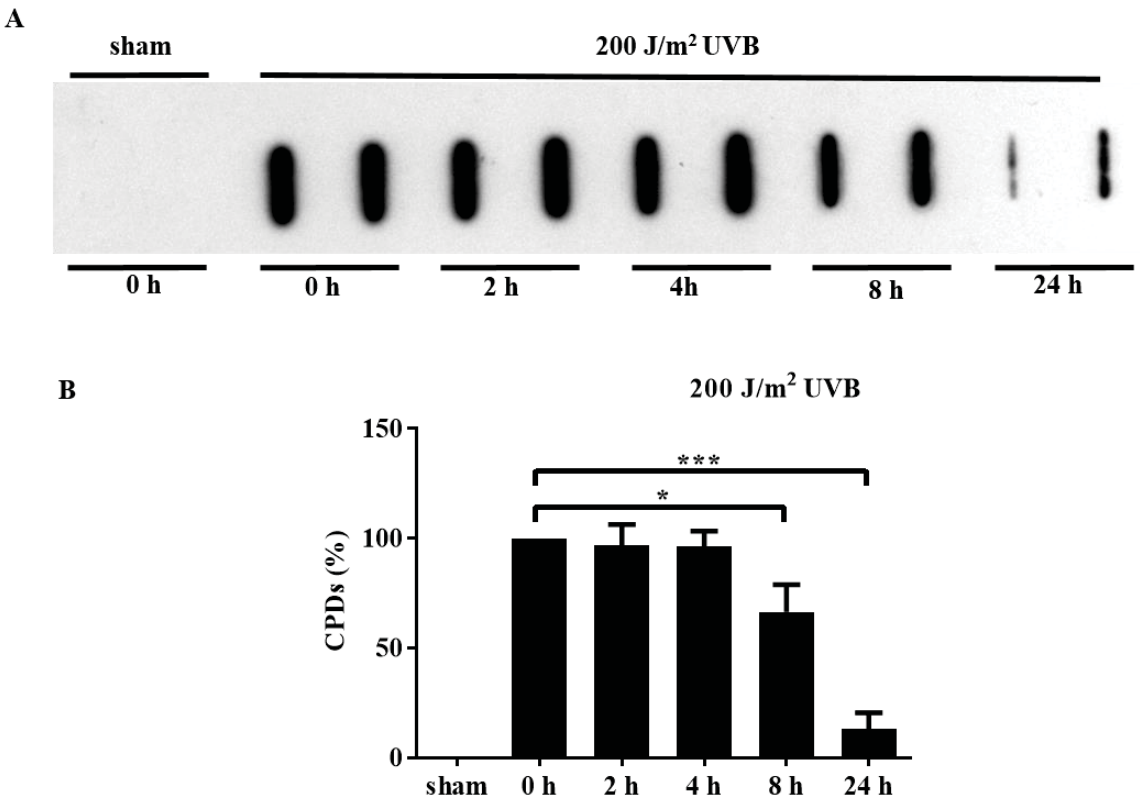

Figure 7 Time-dependent CPD clearance in UVB-irradiated HaCaT cells.
HaCaT cells were irradiated with 200 J/m2 UVB and sham treatment, and DNA was sampled at 0h, 2h, 4h, 8h, and 24h after irradiation. The CPD content in the DNA was measured by Southwestern blot, and normalized to 0h, 200J/m^2 UVB-irradiated samples, (A) Shows the original film of the CPD content in duplicates per each time point and (B) Shows the densitometric analysis of the results. n=4, (***=p<0.001, *=p<0.05) student's t-test.

To investigate the potential impact of AhR signaling on the clearance of UVB-induced CPDs, HaCaT cells were irradiated with 50 J/m^2 and 200 J/m^2 UVB and were subsequently treated with the AhR antagonist MNF. This treatment scenario was chosen to exclude UVB scavenging effects of the flavonoid. The CPD content was determined four hours after irradiation. In comparison to solvent controls, the CPD content was 37.3% and 32.6% lower in MNF-treated cells (Figure 8A and B), which strongly indicates that the chemical inhibition of AhR leads to improved CPD removal.

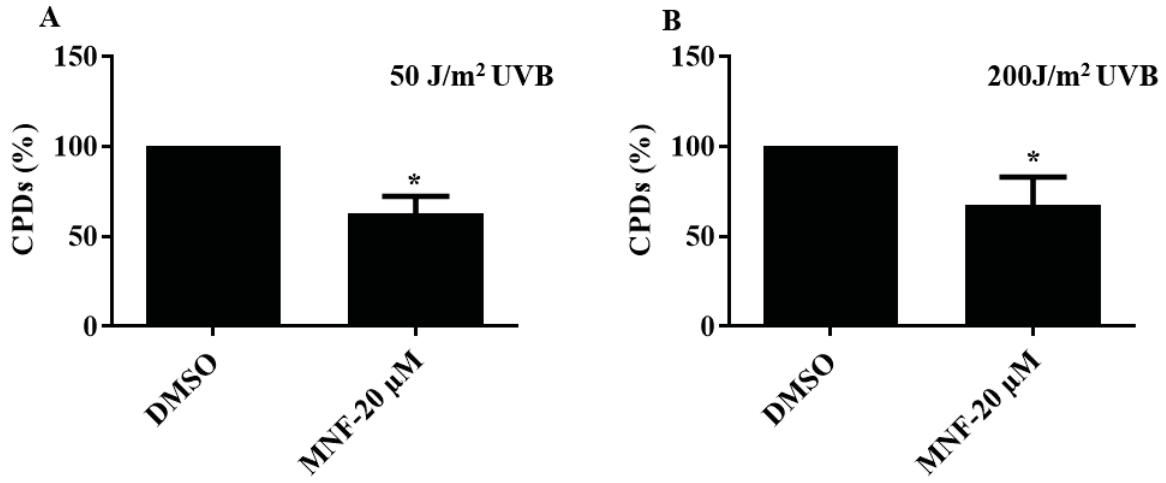

Figure 8 CPDs after UVB irradiation and treatment with AhR antagonist MNF.
HaCaT cells were irradiated with (A) 50 J/m^2, (B) 200 J/m^2 UVB including sham treatment and subsequently exposed to DMSO or 20 µM MNF. CPD content was measured after 4h, a decrease of CPDs in MNF treated cells was detectable when compared to solvent/DMSO treated controls. There were no detectable CPDs in sham treatment. n=3, (*=$p<0.05$) student's t-test

The stably transfected control (HaCaT-ev) and AhR knockdown (HaCaT-shAhR) KC were used. First, the constitutive expressions of AhR and target gene CYP1A1 were determined to verify the successful AhR knockdown. The AhR and CYP1A1 transcript amounts were determined by qPCR. The constitutive expressions of AhR and CYP1A1 in HaCaT-shAhR are significantly lower than that in HaCaT-ev (Figure 9A and B).

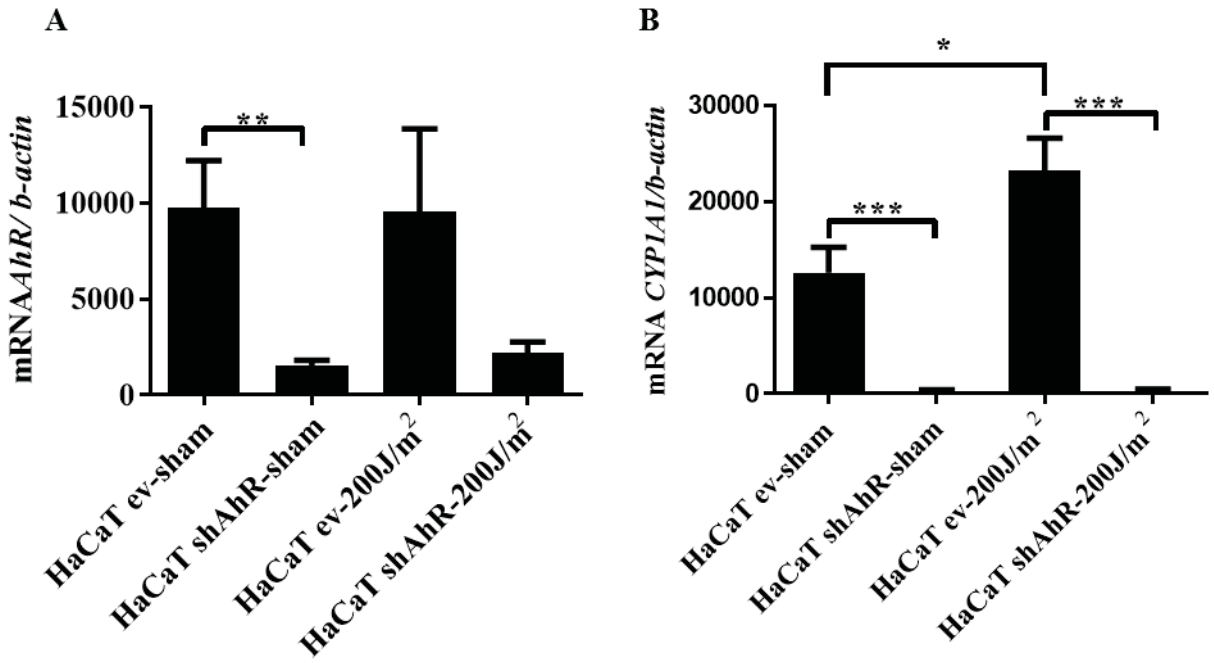

Figure 9 Basal and UVB irradiated gene expression of AhR and CYP1A1 in HACaT-ev and HaCaT-shAhR KC.
Control and AhR knockdown KC were irradiated with 200 J/m^2 UVB, and after 6h, CYP1A1 gene expression was measured, and upregulation of CYP1A1 has seen in HaCat-ev but not in HaCaT-shAhR KC. n=3, (*=$p<0.05$) student's t-test.

Since chemical inhibition of AhR resulted in an improved CPD clearance, we checked whether the genetic inhibition of AhR also contributes to improved CPD removal. To assess this, HaCaT-ev and HaCaT-shAhR cells were irradiated with 200 J/m^2 UVB. After four hours, the amount of CPDs in the respective DNA was analyzed. In line with the reduced CPD clearance in MNF-treated HaCaT cells (Figure 8), the silencing of AhR in HaCaT-shAhR cells led to 37% reduction of CPDs, as compared to that in HaCaT-ev cells (Figure 10)**.** These data demonstrate that AhR inhibits the CPD clearance in UVB-irradiated cells.

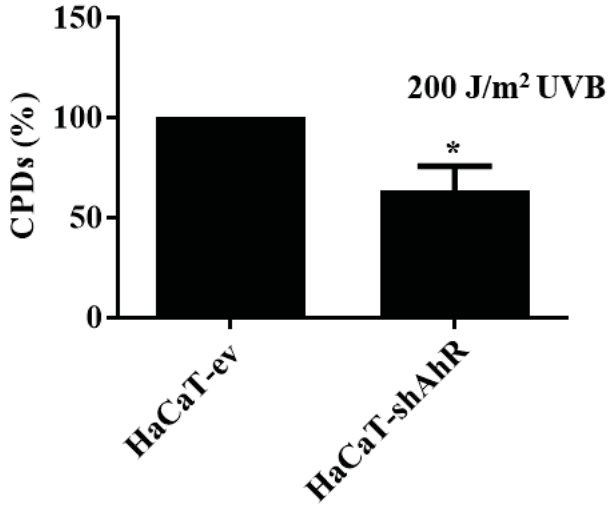

Figure 10 Improved CPD clearance in HaCaT-shAhR KC after UVB irradiation.
HaCaT-ev and HaCaT-shAhR cells were irradiated with 200 J/m^2 UVB, and CPDs were measured after 4h, a decrease of CPDs in HaCaT-shAhR cells was detectable when compared to HaCaT-ev cells. n=3, (*=p<0.05) student's t-test.

Since the loss of function studies (Figures 8 and 10) indicate that AhR inhibition contributes to CPD removal in UVB-irradiated KC, we next analyzed the effect of AhRR on CPD removal in UVB-treated KC. Therefore, AhRR-overexpression experiments were performed. For this, rat AhRR (pAhRR), along with the respective control vector, was transfected into the HaCaT cells using JetPEI transfection reagent.

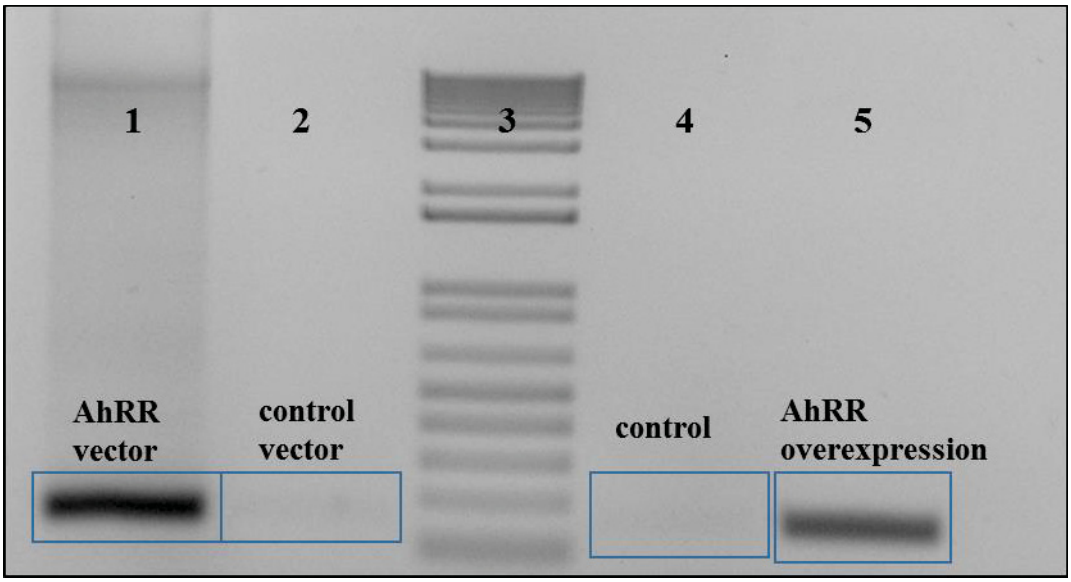

Figure 11 overexpression of rAhRR in HaCaT KC.
HaCaT cells were transfected with control vector (lane 4) or rat AhRR-vector (lane 5). An agarose gel showing PCR of lysed cells transfected with rat AhRR or with control vector.

The efficiency of AhRR overexpression in HaCaT KC was confirmed via PCR (Figure 11). To assess the influence of AhRR on CPD clearance control or AhRR overexpressing KC were irradiated with 200 J/m^2 UVB. After four hours, the DNA was isolated to compare the amount of CPDs between control and AhRR overexpressing KC. More importantly, overexpression of AhRR led to 18% reduction in CPDs four hours after UVB treatment (Figure 12).

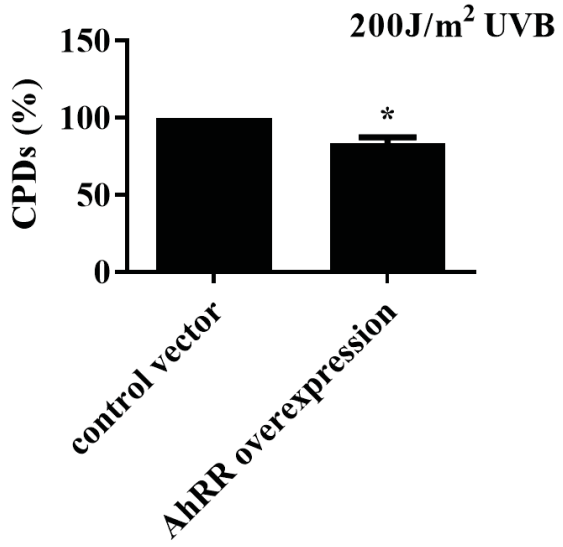

Figure 12 Effect of AhRR overexpression on the clearance of UVB-induced CPDs.
HaCaT cells overexpressing AhRR and control vector were irradiated with 200 J/m^2 UVB and after 4h analyzed for CPDs. The AhRR overexpressing cells showed less CPDs in comparison to control cells. n=3, (*=$p<0.05$) student's t-test.

To assess whether AhR regulates NER by modulating the expression of NER enzymes, HaCaT-ev and HaCaT-shAhR KC were irradiated with 200 J/m^2 UVB. After six hours, the gene expression of some of the enzymes involved in the NER- *XPA, XPB, XPC, XPD, and CSB* was measured (Marteijn et al. 2014). Gene expression analyses of these enzymes revealed that there were no significant AhR-dependent changes in UVB-treated HaCaT-ev and HaCaT-shAhR KC (Figure 13).

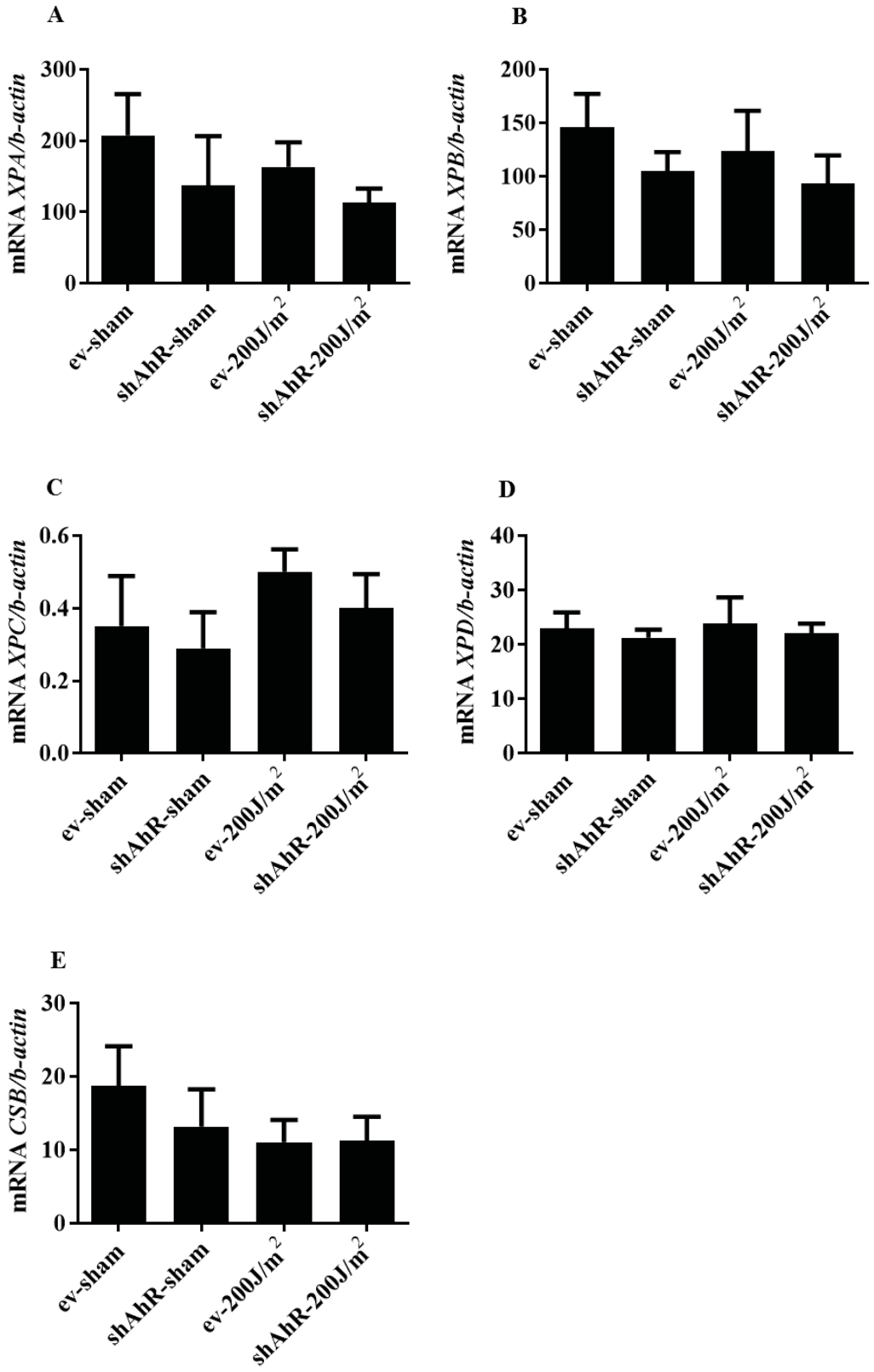

Figure 13 Gene expression levels of NER enzymes in HaCaT-ev and HaCaT-shAhR cells after UVB-irradiation.
HaCaT-ev and HaCaT-shAhR KC were irradiated with 200 J/m^2 UVB and after 6h gene expression analysis of the NER enzymes XPA (A), XPB (B), XPC (C), XPD (D), and CSB (E) were measured. n=3.

For subsequent protein expression measurements of NER enzymes, we irradiated HaCaT-ev and HaCaT-shAhR KC with 200 J/m^2 UVB. After 24 hours, the protein expression of NER enzymes was measured. In line with the qPCR data (Figure 13), the western blot analyses of total proteins revealed that there were no AhR-dependent changes in the expression of NER enzymes (Figure 14).

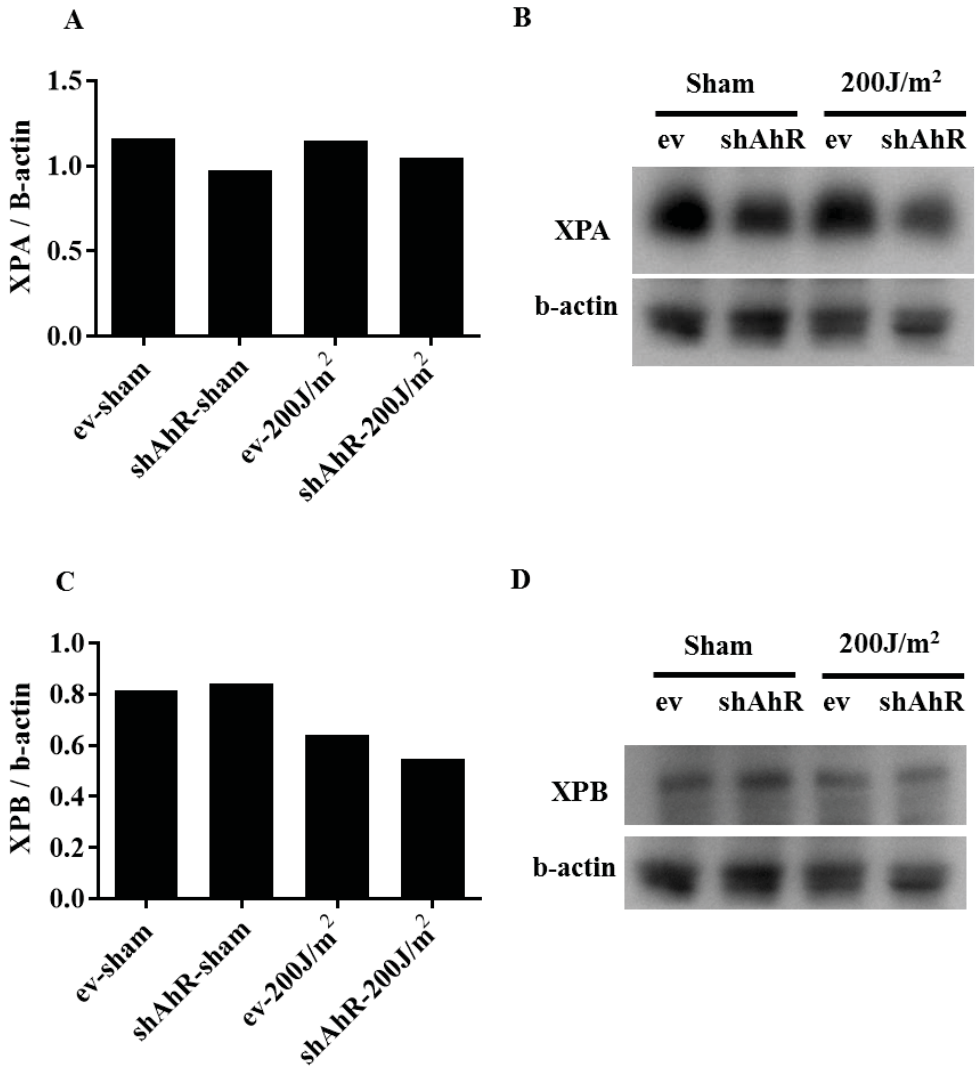

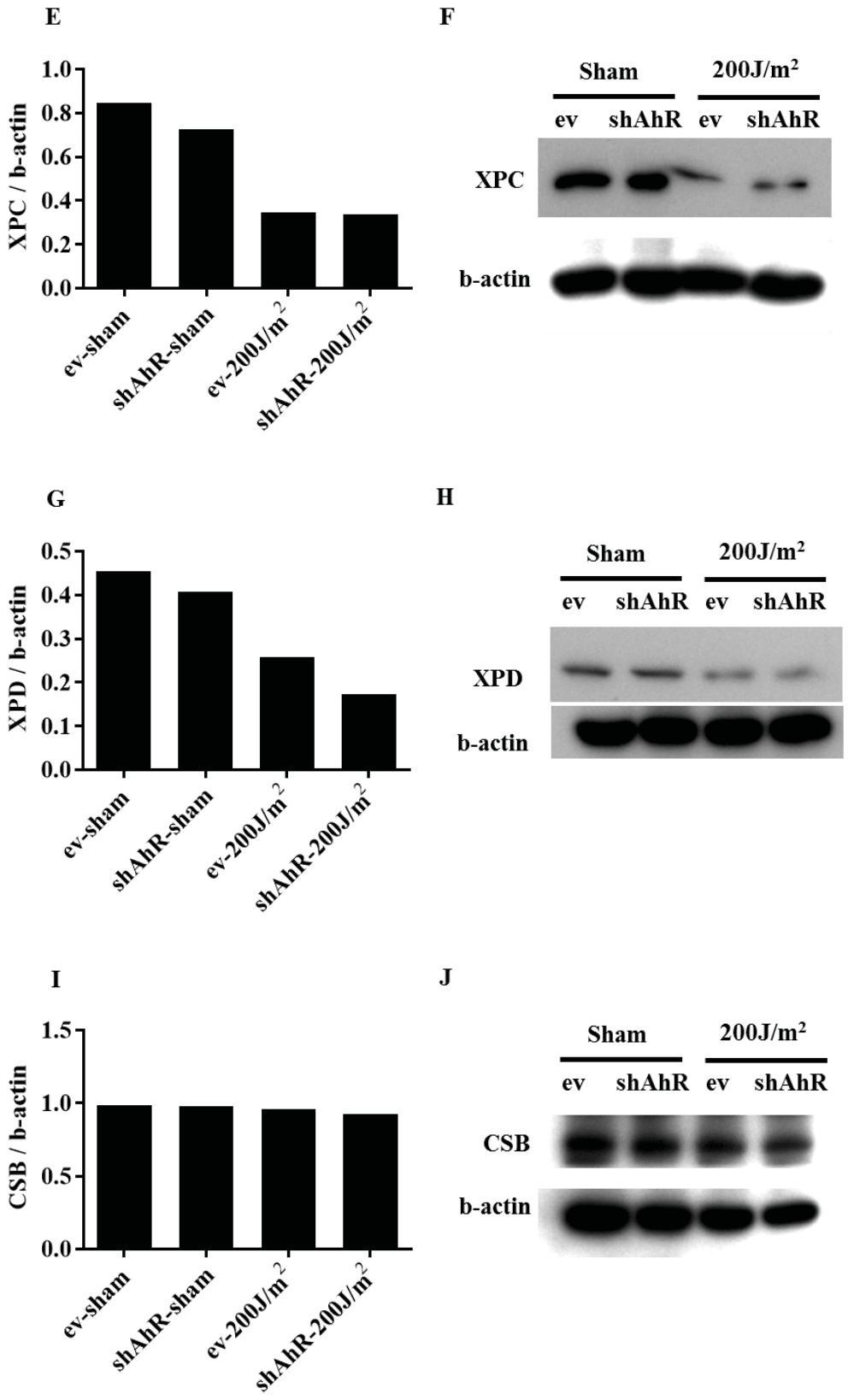

Figure 14 Western blot analysis of NER enzymes in HaCaT-ev and HaCaT-shAhR cells after UVB irradiation.
HaCaT-ev and HaCaT-shAhR KC were irradiated with 200 J/m^2 UVB and after 24 h Protein expression of NER enzymes XPA (A, B), XPB (C, D), XPC (E, F), XPD (G, H), and CSB (I, J) was analyzed. n=1.

While investigating other possible ways in which AhR might influence NER, one of the possible ways to regulate NER is through phosphorylation (Coin et al. 2004). UVB-irradiation activates non-canonical AhR pathway, which involves the c-Src activation of EGFR and downstream ERK phosphorylation (Fritsche et al. 2007). To study the involvement of non-canonical AhR pathway in NER, the phosphorylation of ERK1/2 was analyzed via Western Blot analyses. Indeed, 30 minutes after UVB irradiation of HaCaT cells, there was an increase in phosphorylation of ERK1/2 (Figure 15 Lane 2). As compared to UVB-irradiated DMSO-treated KC, a significant reduction in ERK1/2 phosphorylation was detectable upon inhibition of AhR, Src, EGFR, and MEK. This finding confirms the previous notion that AhR regulates ERK1/2 activation in a Src-EGFR-dependent manner in UVB-exposed KC.

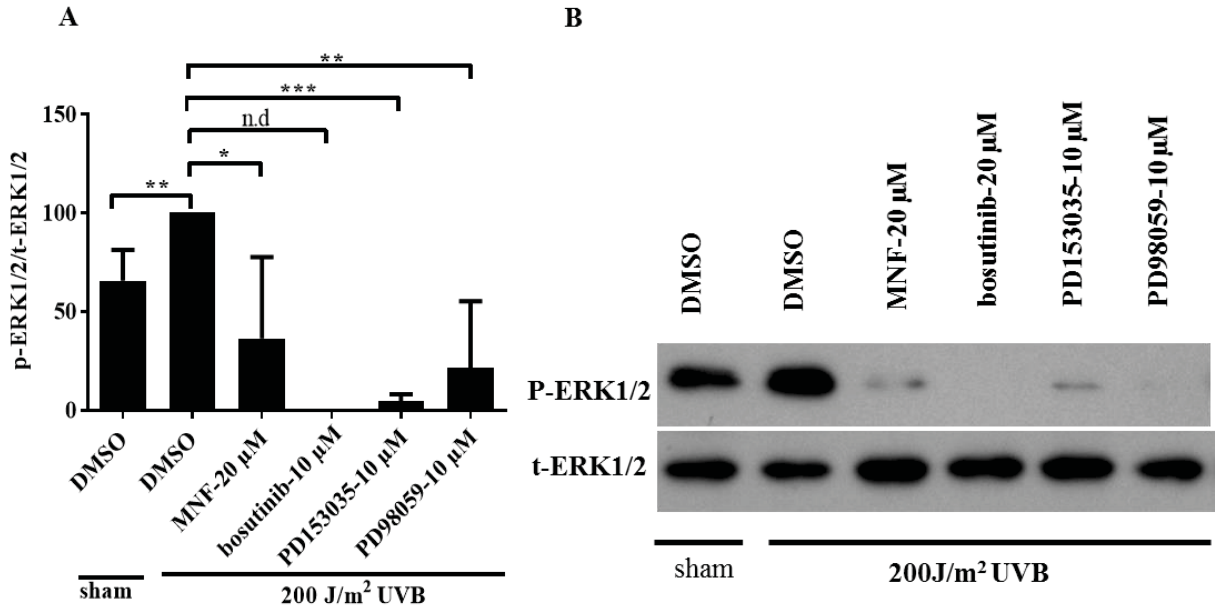

Figure 15 Western blot analysis of ERK1/2 phosphorylation in HaCaT KC after UVB irradiation and subsequent treatment with inhibitors of non-canonical AhR pathway.
HaCaT KC were irradiated with 200 J/m^2 UVB, subsequently treated with inhibitors for AhR (MNF), Src (bosutinib), EGFR (PD153035), MEK (PD98059). After 30 min cells were sampled. Total protein was extracted, and the SDS-PAGE western blot was performed for the phosphorylation of ERK1/2 protein. (A) Shows the densitometric analysis of the results, (B) Shows the original films from the western blot. n=3, (***=p<0.001, **=p<0.01, *=p<0.05), n. d= not detectable, student's t-test.

To further investigate whether the non-canonical AhR pathway is involved in CPD clearance of UVB-irradiated KC, inhibitor experiments targeting the major signalling molecules (c-Src, EGFR, MEK) of the non-canonical AhR signaling cascade have been performed. Indeed, four hours after UVB treatment of HaCaT cells, inhibition of every candidate resulted in an improved CPD removal (Figure 16), indicating non-canonical AhR pathway is involved in the CPD clearance of UVB-irradiated KC.

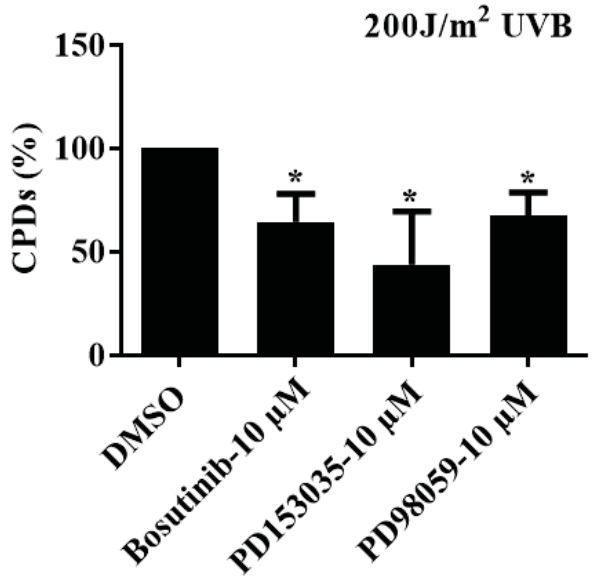

Figure 16 Measurement of CPD content after 200 J/m^2 UVB irradiation and subsequent treatment with inhibitors of non-canonical AhR pathway.
HaCaT cells were irradiated with 200 J/m^2 UVB and subsequently treated with different inhibitors of non-canonical AhR pathway. Bosutinib was used as Src inhibitor, PD153035 was used for EGFR inhibition, and PD98059 was used for MEK inhibition. n=3, (*=$p<0.05$) student's t-test.

To assess the possible clearance of CPD-damaged KC through early apoptosis, we treated HaCaT cells with MNF and Ac-DEVD-CHO (20 µM), an inhibitor of effector caspases. The caspase inhibitor did not affect the MNF-mediated improvement of CPD removal after 200 J/m^2 UVB irradiation (Figure 17), suggesting that AhR may interfere with NER.

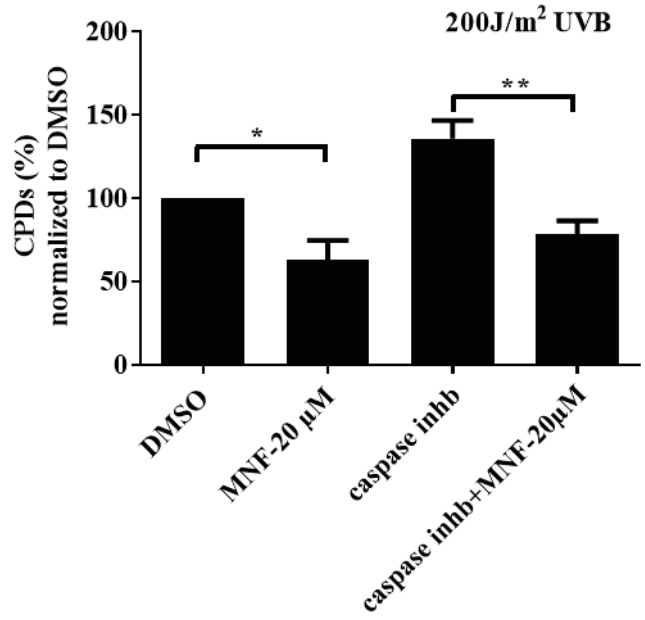

Figure 17 Measurement of CPDs in HaCaT cells irradiated with UVB and subsequently treatment MNF and MNF + caspase inhibitor.
HaCaT cells were irradiated with 200 J/m^2 UVB, subsequently treated with MNF and MNF + caspase inhibitor. After 4h CPD content was measured. n=3, (**=$p<0.01$, *=$p<0.05$) student's t-test

3.2. AhR reduces CPD clearance in an NER-dependent manner

To assess whether the MNF-induced improvement of CPD clearance was NER-dependent, we first silenced the XPA protein. XPA is a DNA repair protein involved in NER; it is responsible for damage verification and acts downstream of XPC and CSB respectively. The XPA protein was transiently silenced by siRNA for XPA in HaCaT cells. Western blotting was used to analyze the efficiency of transfection. The expression of XPA protein in siRNA-XPA KC was 67% lower than that of control siRNA-transfected cells (Figure 18). Next, the XPA-silenced cells were used to assess the CPD clearance in the absence and presence of MNF.

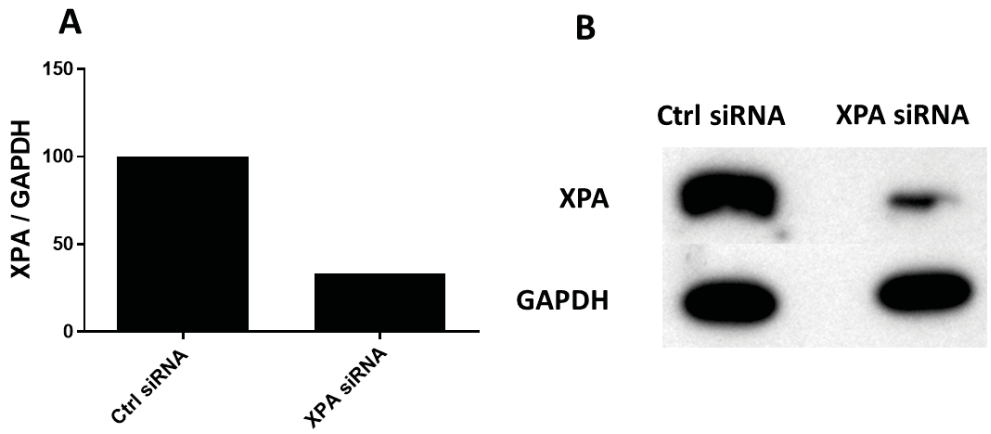

Figure 18 Western blot analysis of XPA protein after siRNA silence.
HaCaT KC were transfected with siRNA for XPA protein along with control siRNA. After 24 h the total protein was isolated, SDS-PAGE western blotting for XPA and housekeeping protein GAPDH was done. This analysis shows that XPA is transiently silenced in KC transfected with siRNA for XPA. (A) Shows the densitometric analysis of the blots and (B) Shows the original films from the western blot.

Control siRNA- and XPA siRNA-transfected HaCaT cells were irradiated with 200 J/m^2 UVB. After irradiation, cells were immediately treated with DMSO or MNF. Four hours later, the analysis of CPD content revealed that the improved removal of CPDs in MNF-treated cells was abolished as soon as XPA was downregulated (Figure 19). This indicates that AhR may directly affect NER-activity.

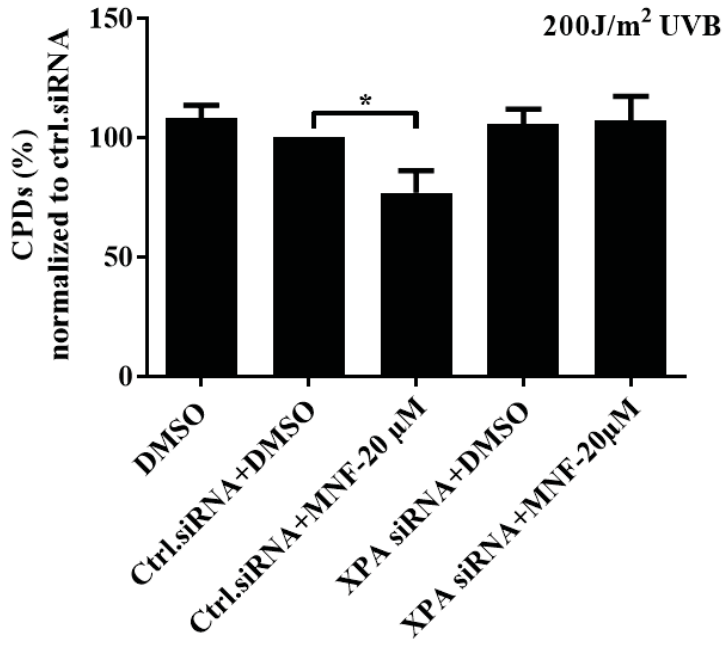

Figure 19 Measurement of CPDs in HaCaT cells transiently silenced for XPA protein after 200 J/m^2 UVB irradiation.
HaCaT cells are transiently silenced for XPA protein with siRNA, followed by 200 J/m^2 UVB exposure and immediately incubated with medium containing DMSO or MNF (20 µM). After 4h CPD content was measured. n=3, (*=p<0.05) student's t-test.

To assess if AhR inhibits GGR, TCR or both sub-pathways of NER respective RNAi studies have been performed. Initially, the expression of XPC was downregulated in HaCaT cells. XPC recognizes DNA damage in the whole genome and initiates GGR. Thus, after confirming efficient knockdown of XPC in HaCaT cells (Figure 20), these cells were further used to analyze the effect of MNF on CPD clearance.

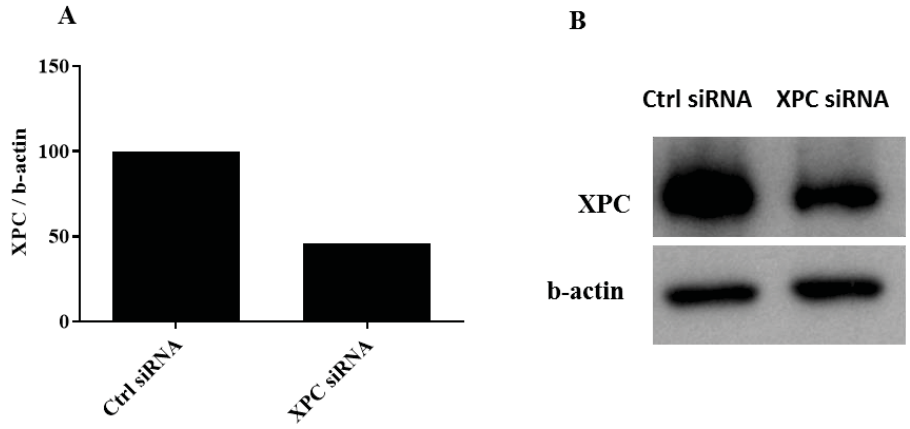

Figure 20 Western blot analysis for XPC protein after siRNA silence.
HaCaT cells were transfected with siRNA for XPC protein along with the control siRNA. After 24 h total protein was isolated and western blotting analysis was done for XPC and housekeeping protein β-actin. This analysis shows transient knockdown of XPC protein in HaCaT cells. (A) Shows the densitometric analysis of blot and (B) Shows the original film from the protein expression analysis.

Control and XPC-knockdown HaCaT cells were irradiated with 200 J/m^2 of UVB. After irradiation, cells were immediately treated with DMSO or MNF. Four hours later, analysis of CPD content revealed that 33% faster removal of CPDs in MNF-treated KC was abolished, as soon as XPC was downregulated (Figure 21), indicating that AhR is capable of affecting GGR activity.

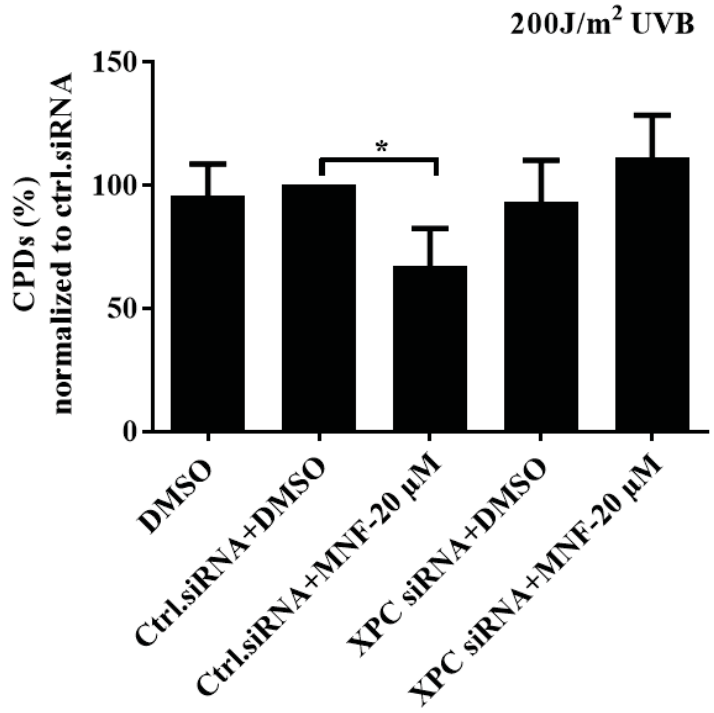

Figure 21 Measurement of CPDs in HaCaT KC transiently silenced for XPC protein after 200 J/m^2 UVB irradiation.
HaCaT cells were silenced for XPC protein with siRNA, and then they were irradiated with 200 J/m^2 UVB and immediately incubated with medium containing DMSO or MNF (20 µM). After 4h the cells were sampled for DNA and CPD content was measured. n=3, (*=p<0.05) student's t-test.

To investigate if AhR also alters TCR, the CSB protein was transiently silenced. CSB recognizes DNA damage-stalled RNA polymerase to activate TCR. Thus, after confirming efficient knockdown of CSB in HaCaT cells (Figure 22), these cells were further used to analyze the effect of MNF on the CPD clearance.

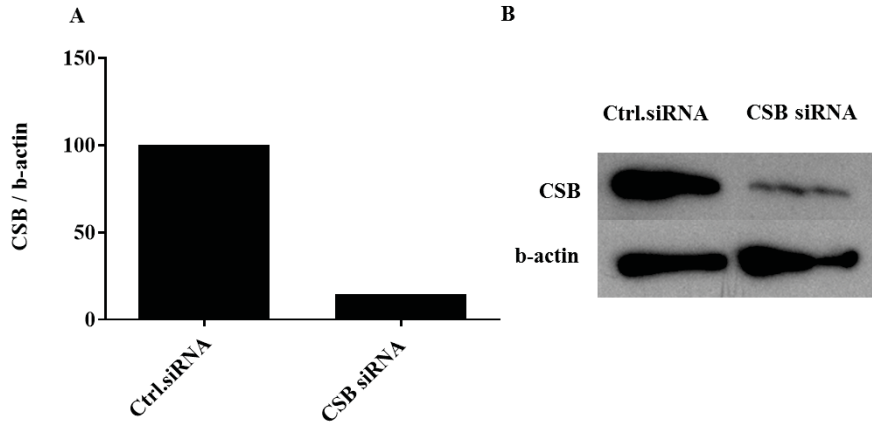

Figure 22 Western blot analysis of CSB protein after siRNA silence.
HaCaT cells were transfected with siRNA CSB along with the control siRNA. After 24 h total protein was isolated and protein expression was analyzed for CSB and housekeeping protein β-actin by western blot. (A) Shows the densitometric analysis of blots and (B) Shows the original film from the protein expression analysis.

Control and CSB-knockdown HaCaT KC were irradiated with 200 J/m^2 UVB. After irradiation, cells were immediately treated with DMSO or 20 µM of MNF. Four hours later, analysis of CPD content revealed that the 28% improvement in CPD removal in MNF-treated KC still present after CSB knockdown (Figure 23), This points to the idea that AhR may not regulate the activity of TCR.

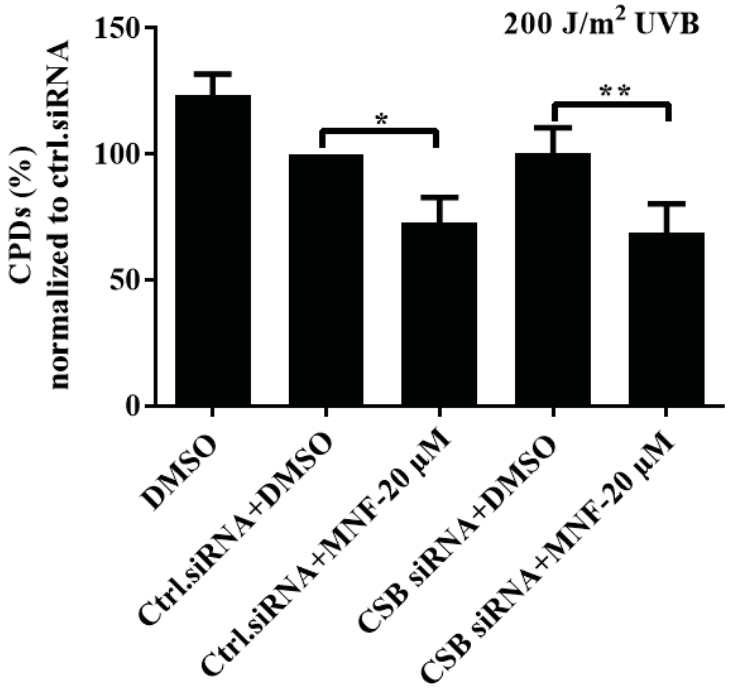

Figure 23 Measurement of CPDs in HaCaT cells transiently silenced for CSB protein after 200 J/m^2 UVB irradiation.
HaCaT cells were silenced for CSB protein with siRNA, and then they were irradiated with 200 J/m^2 UVB and subsequently incubated with medium containing DMSO or MNF (20 µM). After four hours, the cells were sampled for DNA, and CPD content was measured. n=3, (**=p<0.01, *=p<0.05) student's t-test.

In summary, these results show that AhR negatively regulates GGR, but not TCR. As GGR activity is known to be closely linked to cell-cycle arrest (Demetriou et al. 2012), we next assessed whether the improved CPD clearance of MNF treatment is still present in non-proliferating (confluent) cells. Indeed, the MNF treatment of non-proliferating HaCaT cells did not improve the UVB-induced CPD clearance (Figure 24).

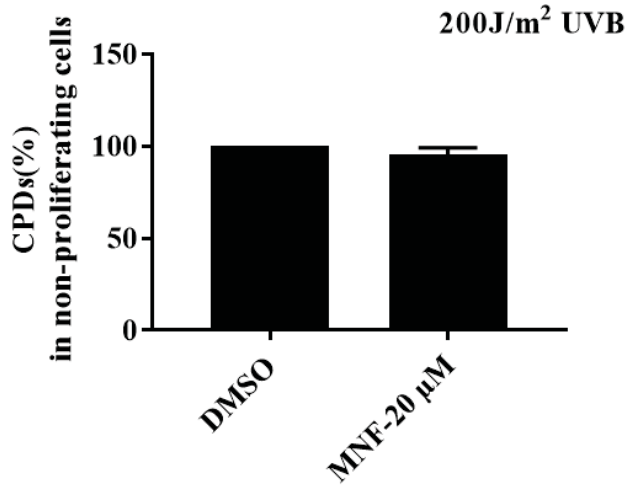

Figure 24 CPD measurement in non-proliferating HaCaT cells after UVB irradiation.
HaCaT cells were cultured in 6 well plates till they reach 100% confluent. Then these cells were irradiated with 200 J/m^2 UVB and subsequently treated with MNF (20 µM) or DMSO. After four hours CPD content was measured. n=3.

To further test the hypothesis that the enhancement in GGR activity upon MNF treatment is due to alterations in the cell cycle, HaCaT KC were treated with roscovitine, a cyclin-dependent kinase (CDK) inhibitor, and analyzed for CPD content after exposure to 200 J/m^2 UVB. Four hours after UVB irradiation, there was an improvement in CPD removal (Figure 25). This indicates that CDK inhibits improved CPD removal in HaCaT KC.

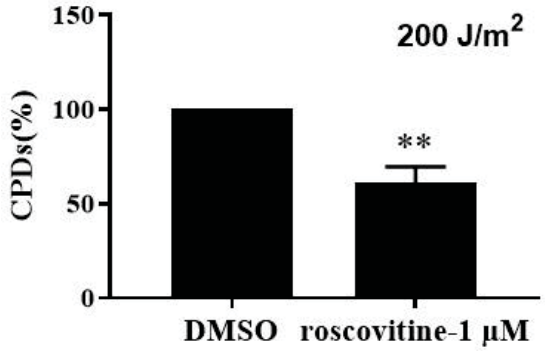

Figure 25 CPD content in HaCaT cells after UVB irradiation and treatment with CDK inhibitor.
HaCaT cells were irradiated with 200 J/m^2 UVB and subsequently exposed to DMSO or 1 µM roscovitine. CPDs were measured after 4h. A. n=3, (**=p<0.01) student's t-test.

Next, in order to test whether biological CDK inhibitor p27^{KIP1} has an effect similar to the chemical CDK inhibitor (Frauenstein et al. 2013), p27^{KIP1} was transiently silenced by RNAi. The efficiency of p27^{KIP1} silencing was analyzed by western blotting (Figure 26). These cells that were transiently silenced for p27^{KIP1} were used to analyze the CPD removal.

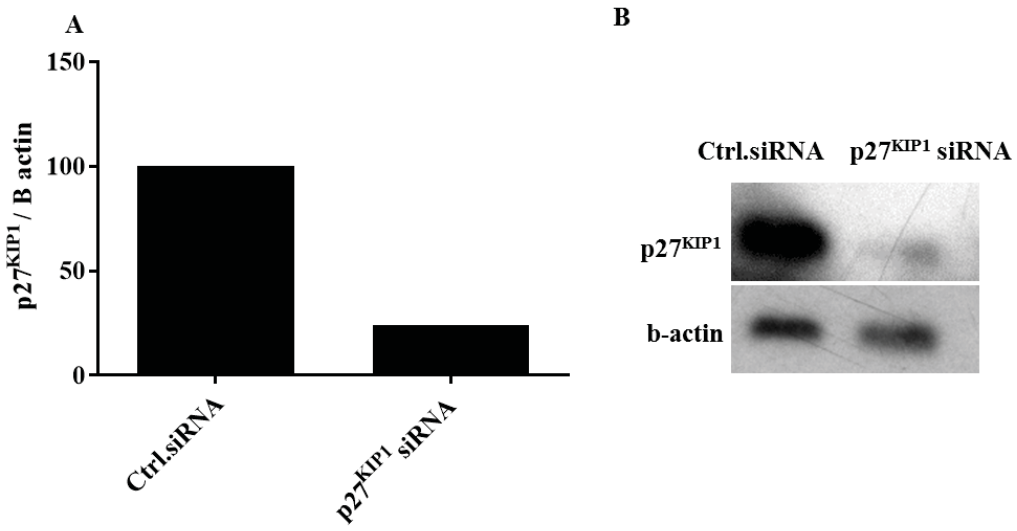

Figure 26 Western blot analysis confirming the siRNA p27^{KIP1} knockdown.
HaCaT cells were transfected with siRNA for p27^{KIP1} protein or with control siRNA. After 24h total protein was isolated and protein expression analysis was performed for p27^{KIP1} and housekeeping protein β-actin. This analysis shows that p27^{KIP1} protein was transiently silenced in transfected cells (siRNA for p27$^{KIP1)}$. (A) Shows the densitometric analysis of blots and (B) Shows the original films from the protein expression analysis.

The p27^{KIP1}-silenced cells were irradiated with 200 J/m^2 of UVB along with the controls. In contrast to control cells, the p27^{KIP1} knockdown abolished the MNF mediated enhancement of CPD removal (Figure 27). This strongly indicates that AhR-mediated inhibition of GGR activity happens by modulating p27^{KIP1}.

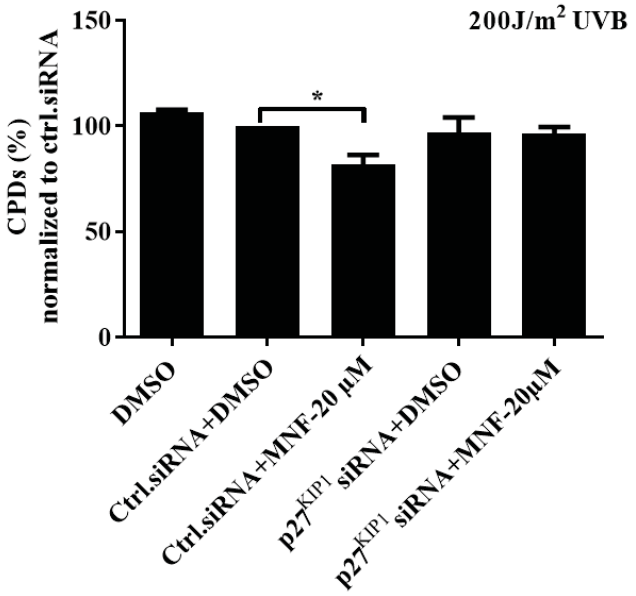

Figure 27 Measurement of CPDs in p27^{KIP1} knockdown HaCaT cells after 200J/m^2 UVB radiation.
HaCaT cells were silenced for p27^{KIP1} protein with siRNA and irradiated with 200 J/m^2 UVB. Immediately after UVB exposure, cells were incubated with medium containing DMSO or MNF-20 µM. After 4h the DNA was isolated to measure CPDs. n=3, (*=p<0.05) student's t-test.

To confirm the critical role of $p27^{KIP1}$ in NER, the transient overexpression of $p27^{KIP1}$ in HaCaT cells was done. This resulted in the improved removal of CPDs four hours after UVB irradiation (Figure 28), indicating that the $p27^{KIP1}$ protein level positively correlated with NER activity.

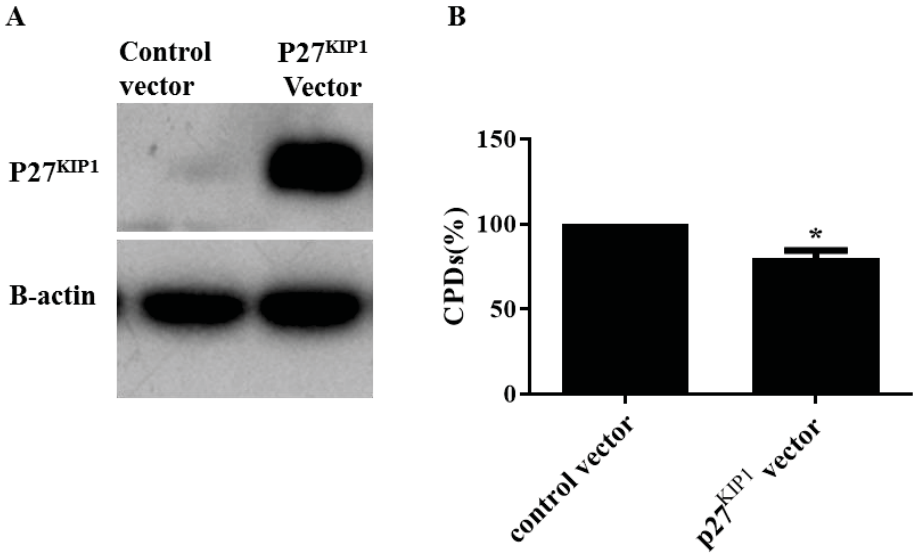

Figure 28 Measurement of CPDs in $p27^{KIP1}$ overexpressing HaCaT KC after UVB irradiation. HaCaT cells were transfected with control vector or $p27^{KIP1}$. (A) Western blot of cells transfected with $p27^{KIP1}$ to control overexpression. (B) $p27^{KIP1}$ overexpressed cells have fewer CPDs in comparison to control vector cells. n=3, (*=$p<0.05$) student's t-test.

3.3. AhR affects UVB-induced apoptosis

The results above show that AhR inhibition significantly accelerates CPD-removal by amplifying GGR. The accelerated repair of CPDs should rescue the damaged cells from apoptosis (Chigancas et al. 2002), however, as previously reported (Frauenstein et al. 2013), the opposite, i.e. an enhanced occurrence of apoptosis in AhR-compromised KC, was observed.

To investigate whether chemical inhibition of AhR modulates the UVB-induced apoptosis, HaCaT cells were irradiated with 200 J/m^2 of UVB. After irradiation, the cells were treated with MNF or DMSO. After 24 hours of treatment, cells were harvested for Annexin V/propidium iodide staining and dead cells were determined via FACS analysis. The chemical AhR inhibition led to an increased UVB-induced apoptosis (Figure 29).

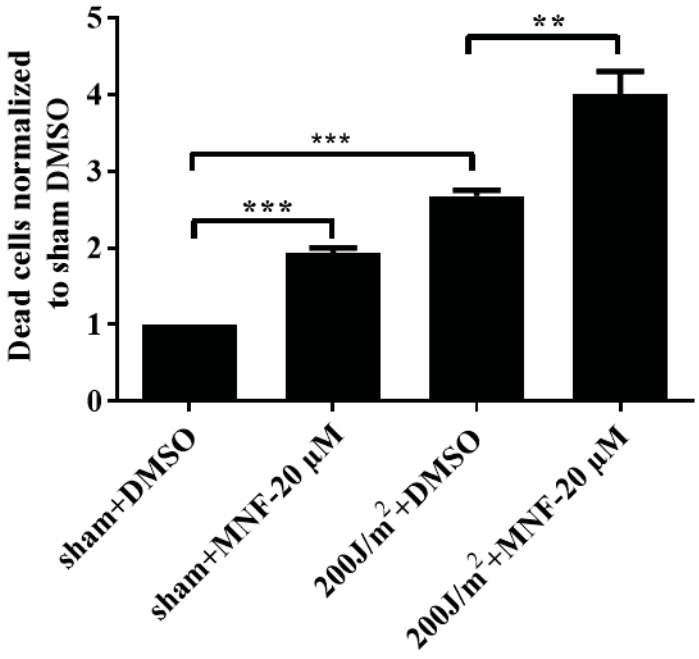

Figure 29 Measurement of apoptosis in HaCaT cells after UVB irradiation and treatment with MNF.
HaCaT cells were irradiated with 200 J/m^2 UVB. After irradiation, they were treated with MNF (20 µM) or DMSO. 24h after treatment the cells were harvested, stained with annexin V/propidium iodide and analyzed for apoptosis. n=3, (***=p<0.001, **=p<0.01) student's t-test.

Further, to investigate if sh-RNA-mediated AhR inhibition has an influence on UVB-induced apoptosis, HaCaT-ev and HaCaT-shAhR were irradiated with 200 J/m^2 UVB. Twenty-four hours after irradiation, the cells were harvested for FACS analyses. AhR inhibition resulted in an increased occurrence of apoptosis (Figure 30).

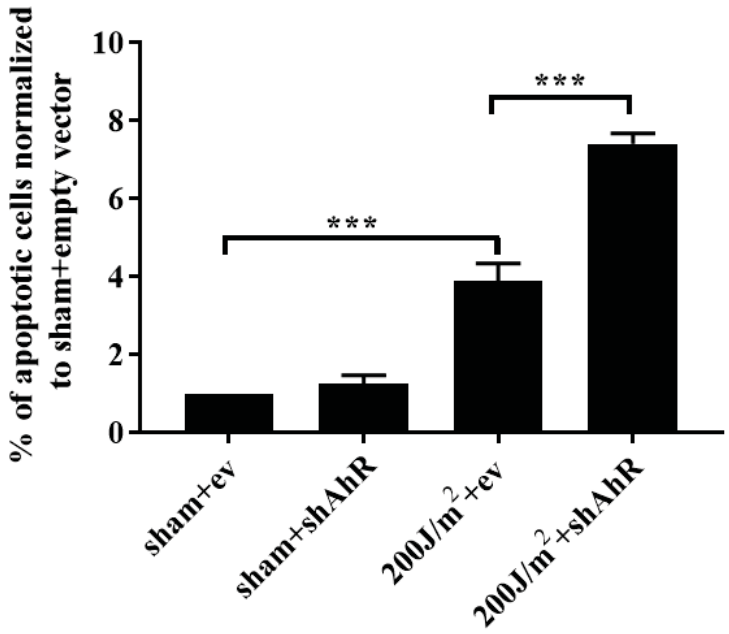

Figure 30 Measurement of apoptosis in HaCaT-shAhR KC after UVB-irradiation.
HaCaT-ev and HaCaT-shAhR were irradiated with 200 J/m^2 UVB. Twenty-four hours after irradiation the cells were harvested, stained with annexin V/propidium iodide and analyzed for apoptotic cells. n=3, (***=$p<0.001$) student's t-test.

We investigated the effect of AhRR overexpression on apoptosis in UVB-irradiated HaCaT cells. For this, the cells were manipulated to overexpress AhRR. AhRR-overexpressing cells were irradiated with 200 J/m^2 UVB, and after 24 hours the cells were analyzed for apoptosis via FACS analyses. As expected, overexpression of AhRR resulted in increased apoptosis after UVB irradiation (Figure 31).

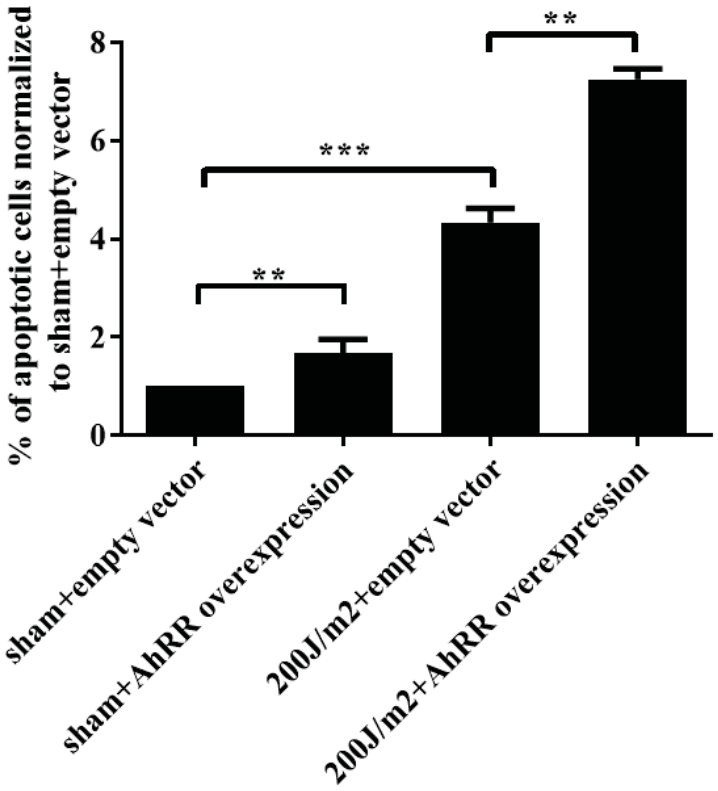

Figure 31 Measurement of apoptosis in HaCaT cells transiently overexpressing for AhRR after UVB irradiation.
HaCaT cells overexpressing AhRR were irradiated with 200 J/m^2 UVB. 24h after irradiation the cells were harvested, stained with annexin V/propidium iodide and analyzed for apoptosis. n=3, (***=p<0.001, **=p<0.01) student's t-test.

In summary, the data from Sections 3.3.1 and 3.3.2 clearly demonstrate that AhR inhibits apoptosis in UVB-treated KC. This is in line with the findings of Frauenstein et al. (Frauenstein et al. 2013).

According to Frauenstein et al. apoptosis was caused by impaired AhR signaling due to the reduction of CHK1 levels in KC (Frauenstein et al. 2013). DNA double-strand breaks are known to induce apoptosis (Lips and Kaina 2001). Therefore, to analyze whether apoptosis is due to double-strand breaks, the expression of γH2AX was measured after MNF treatment, which is a marker for DNA double-strand breaks (Kuo and Yang 2008). HaCaT cells were irradiated with 200 J/m^2 UVB and subsequently treated with MNF. After 18 hours, the cells were harvested and total protein was extracted. Western blot analyses were performed for the protein γH2AX. Significant up-regulation of γH2AX in MNF-treated samples, as observed in

comparison to control cells (Figure 32), indicate that AhR inhibition may be associated with DNA double-strand break formation.

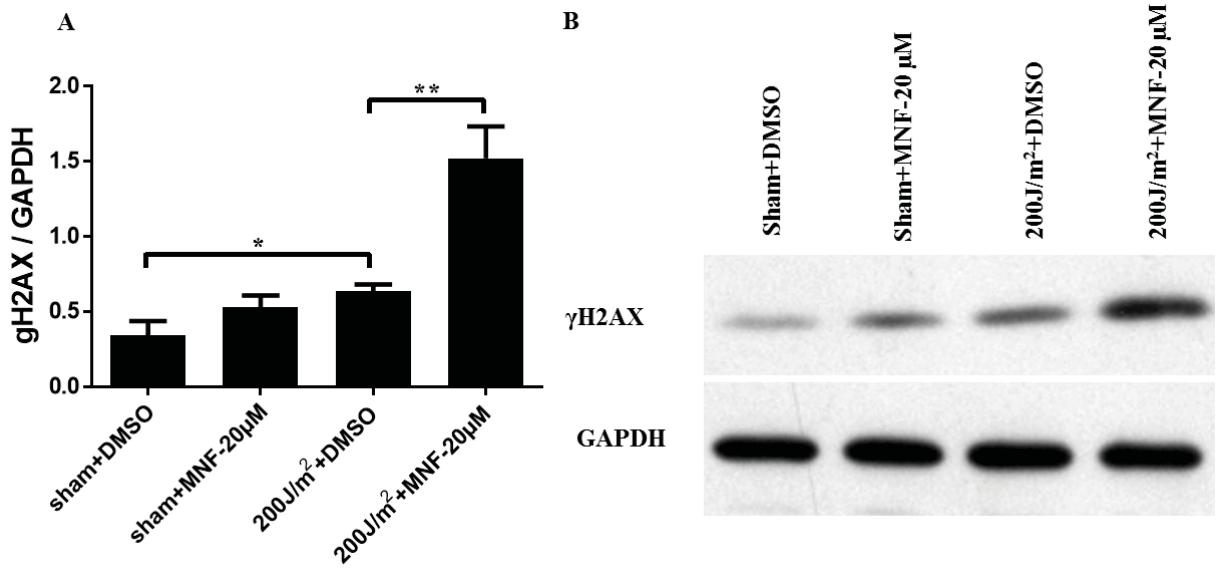

Figure 32 Western blot analyses of γH2AX in MNF-treated HaCaT cells.
HaCaT cells were irradiated with 200 J/m^2 UVB. Immediately after irradiation, the cells were treated with AhR antagonist MNF or DMSO. After 16 h the cells were harvested, and protein expression analysis was performed for the phosphorylation of γH2AX protein. (A) Shows the densitometric analysis of the results. (B) Shows the original films from the western blot. n=3, (**=p<0.01, *=p<0.05) student's t-test.

To confirm the double-strand break generation by AhR inhibition in KC after UVB irradiation with a second method, neutral comet assays were performed (Olive et al. 1993). HaCaT cells were irradiated with 200 J/m^2 UVB. Immediately after UVB irradiation, cells were treated with MNF (20 µM) or DMSO. After 18 hours, the cells were harvested for neutral comet assay to measure the double-strand breaks in the DNA. The tail moment was measured as an index for DNA double-strand breaks. After 18 hours, the average tail moment increased significantly in UVB-irradiated MNF-treated cells compared to controls (Figure 33). This finding strongly indicates that AhR inhibition triggers the formation of DNA double-strand breaks. AhR inhibition is associated with a reduced CHK1 expression (Figure 34).

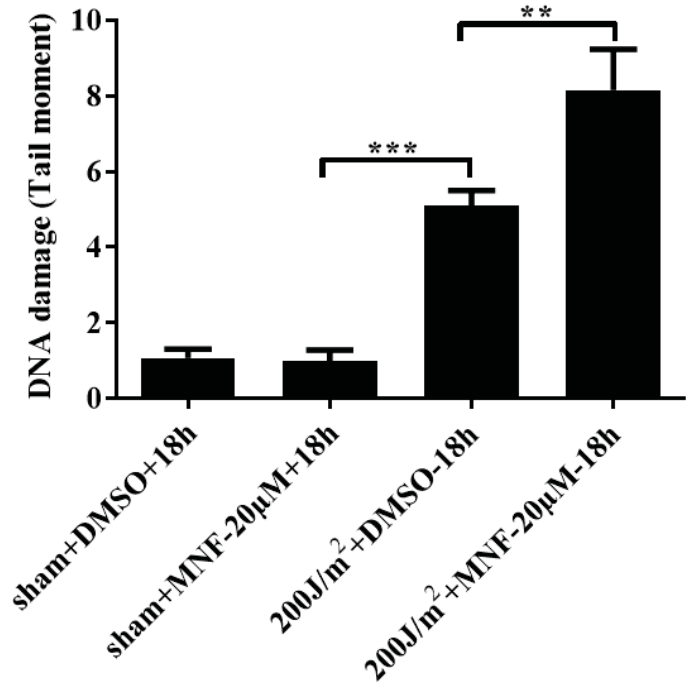

Figure 33 Measurement of DNA damage in HaCaT cells irradiated with UVB and subsequent treatment with MNF.
HaCaT cells were irradiated with 200J/m^2. Immediately after irradiation, they were treated with AhR antagonist MNF (20 µM). After 18h neutral comet assay was performed. The cells were analyzed for the tail moments of the comets as an indicator of double strand breaks. n=3, (***=p<0.001, **=p<0.01) student's t-test.

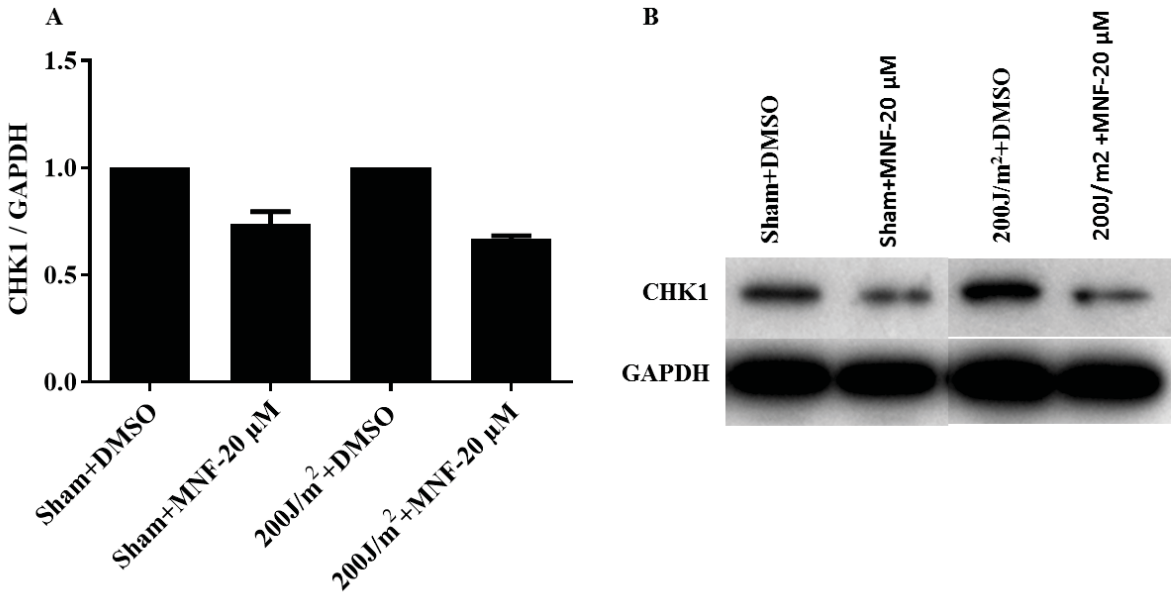

Figure 34 CHK1 protein expression in HaCaT cells after UVB irradiation and treatment with MNF.
HaCaT cells were irradiated with 200 J/m^2 UVB, immediately treated with AhR antagonist MNF or DMSO. After 18 h the cells were sampled, total protein was extracted, and CHK1 protein expression was assessed. (A) Shows the densitometric analysis of the western blot results, where there is less CHK1 in MNF treated samples. (B) Shows the original films from the western blot. n=2.

We next asked whether AhR inhibition also enhances apoptosis in UVB- irradiated malignant cells. Therefore, we performed mechanistic studies in two human cutaneous SCC cell lines A431 (Giard et al. 1973) and SCL-1 (Boukamp et al. 1982), which differ in their constitutive AhR expression (Figure 35 A, B, C). In comparison to normal human epidermal KC (NHEK), A431 cells, but not SCL-1 cells, exhibit a significantly higher AhR expression level at both mRNA and protein level. The basal ARNT mRNA levels did not differ between the primary KC and the KC-derived cancer cell lines (Figure 35D).

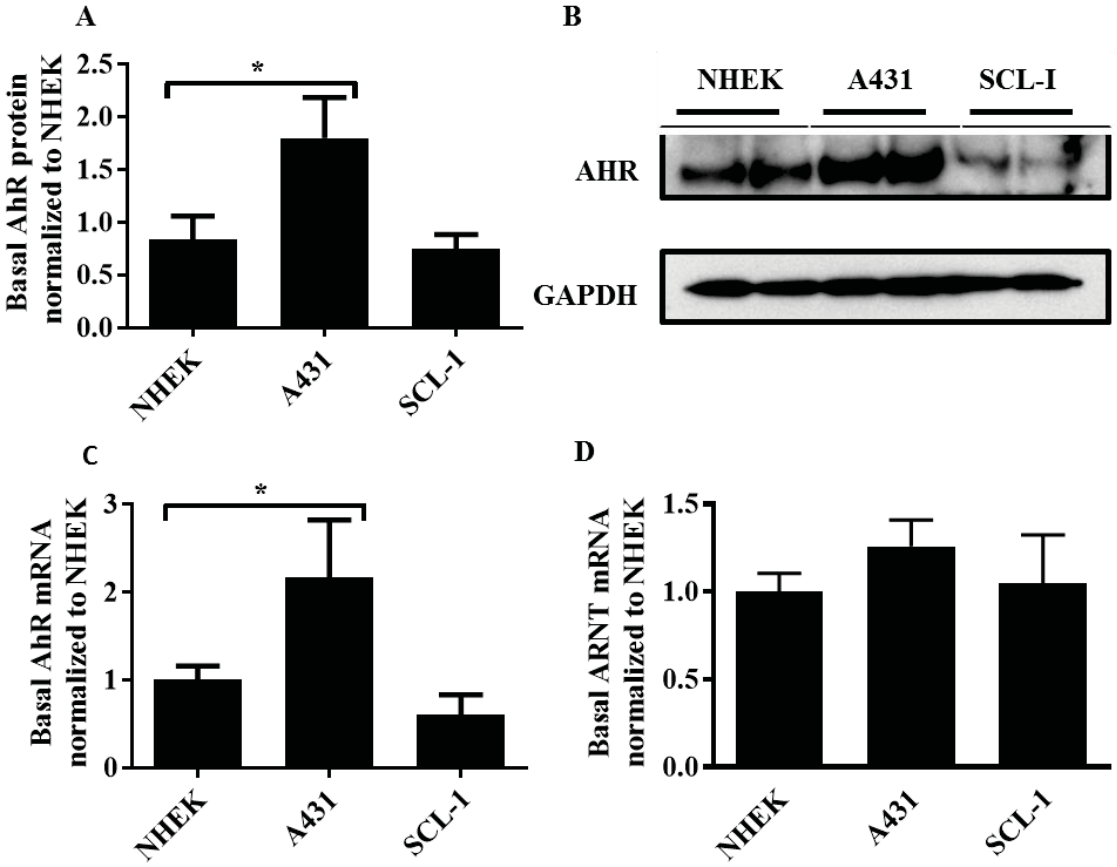

Figure 35 Basal AhR protein and mRNA level of AhR and ARNT in A431 and SCL-1 cells and NHEKs.
Basal protein and mRNA levels of AhR in NHEK, A431, and SCL-1 cells. (A) Densitometric analysis of basal AhR protein from NHEK, A431, and SCL-1 cells. (B) A representative of original film of western blot. (C) Basal AhR mRNA levels in NHEK, A431, and SCL-1 cells. n=3, (*=$p<0.05$) student's t-test.

To analyze the influence of AhR inhibition for UVB-induced apoptosis, AhR expression was transiently silenced in SCL-1 and A431 SCC cells by RNAi. Twenty-four hours after transfection western blot analysis was done to monitor AhR protein expression. The expression of AhR was reduced by transfecting the cell lines with 50 nM AhR siRNA (Figure 36).

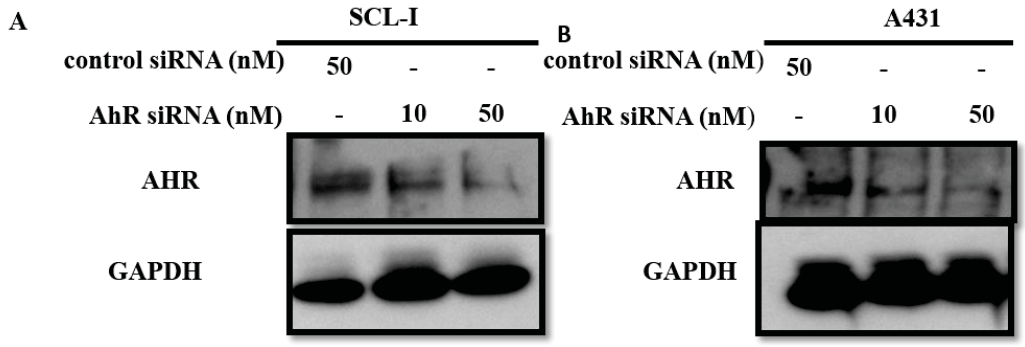

Figure 36 Western blot analysis of AhR protein after siRNA transfection in A431 and SCL-1 SCC cell lines.
A431 and SCL-1 cells were transfected with AhR-targeted siRNA. (A) Protein expression of AhR in SCL-1 cells, 24h after siRNA transfection. (B) Protein expression of AhR in A431 cells, 24h after siRNA transfection.

For the subsequent apoptosis measurements, AhR was either transiently silenced with siRNA or blocked with MNF (20 μM). Both strategies led to an increased cleavage of the caspase substrate PARP-1 upon irradiation of A431 (Figure 37) and SCL-1 (Figure 38) cells with 200 J/m^2 UVB. This indicates that AhR inhibition sensitizes A431 and SCL-1 cells to UVB-induced apoptosis.

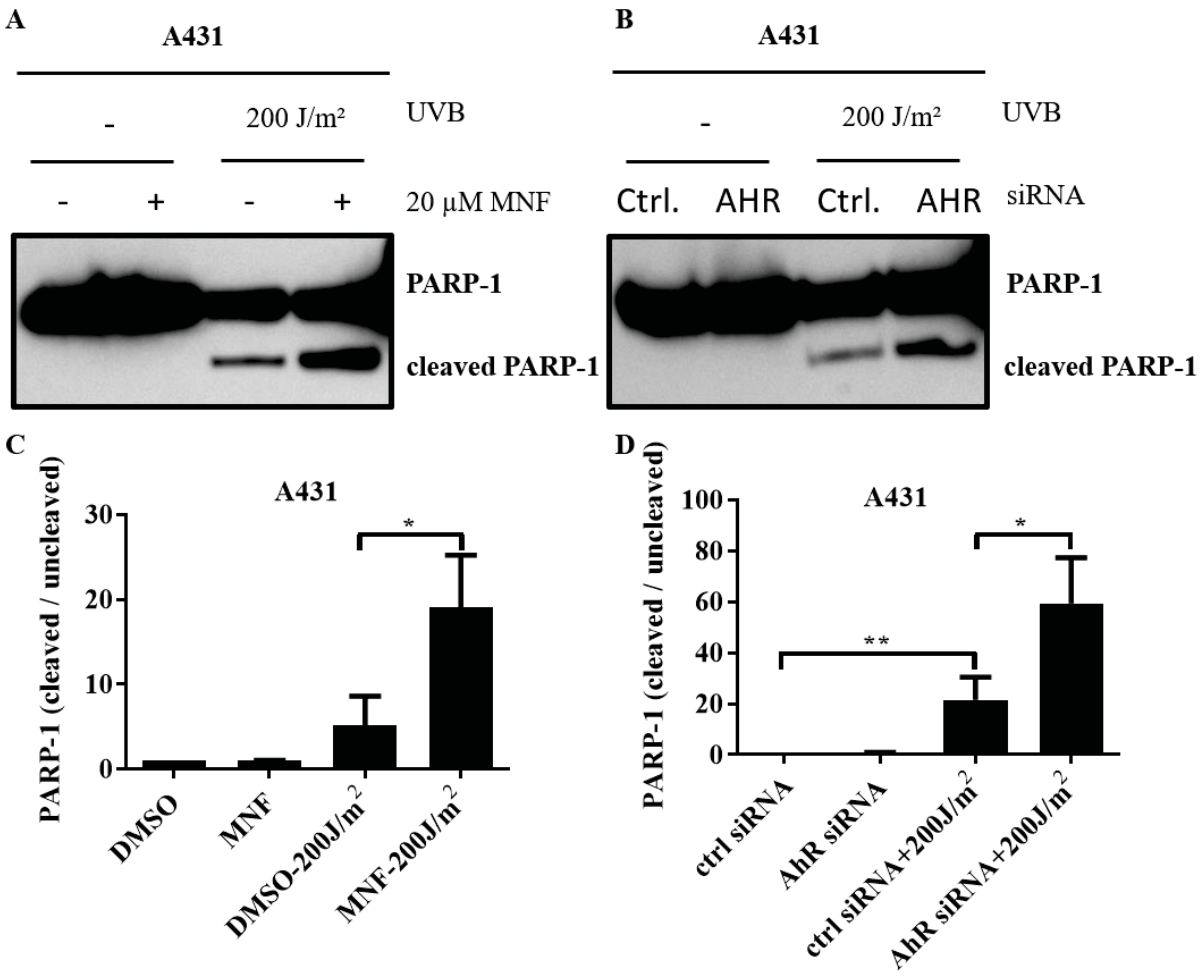

Figure 37 Western blot analyses of PARP-1 in HaCaT KC after treatment with MNF.
A431 cells were transiently silenced for AhR and irradiated with 200 J/m^2 UVB and treated with MNF. After 24h SDS-PAGE electrophoresis was done to detect PARP-1. (A) Western blot analysis of PARP-1 and (C) Densitometric analysis of PARP-1 after UVB irradiation and treatment with MNF (20 µM). (B) Western blot analysis of PARP-1 cleavage and (D) Densitometric analysis of PARP-1 transiently knockdown siRNA AhR A431 cells after 200 J/m^2 UVB irradiation. n=3, (**=$p<0.01$, *=$p<0.05$) student's t-test.

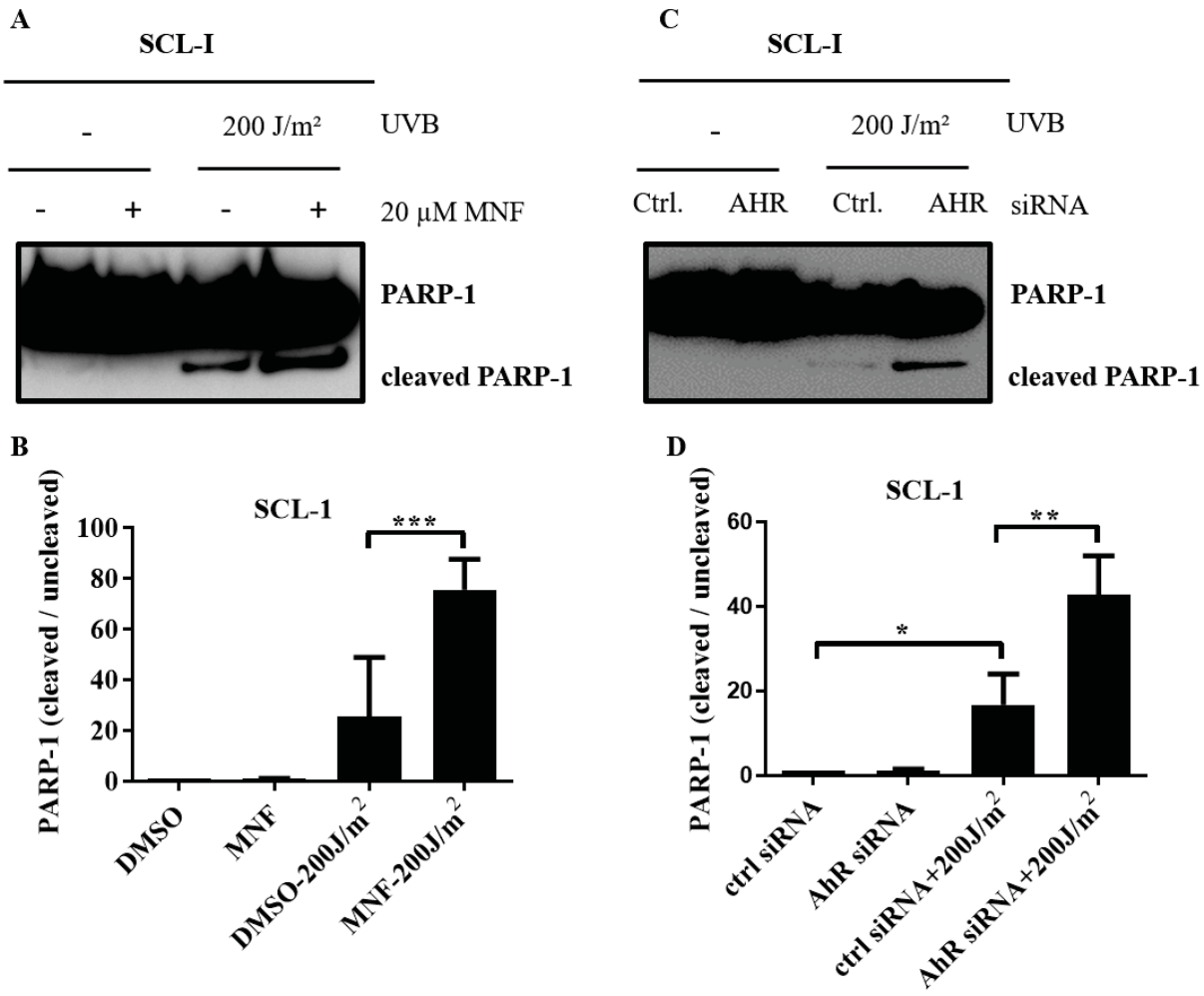

Figure 38 Inhibition of AhR enhances UVB-induced apoptosis in SCL-1 cells.
SCL-1 cells were transiently silenced for AhR and irradiated with 200 J/m^2 UVB or treated MNF after irradiation with 200 J/m^2 UVB. After 24h and SDS-PAGE electrophoresis was done to detect PARP-1. (A) Western blot analysis of PARP-1 and (C) Densitometric analysis of PARP-1 after UVB irradiation and treatment with MNF-20 µM. (B) Western blot analysis of PARP-1 and (D) Densitometric analysis of PARP-1 in transiently knockdown siRNA AhR SCL-1 cells after 200 J/m^2 UVB irradiation. n=3, (***=p<0.001, **=p<0.01, *=p<0.05) student's t-test.

In summary, chemical and siRNA-mediated inhibition of AhR sensitizes human cutaneous SCC cell lines to UVB-induced apoptosis.

AhR expression was transiently silenced in A431 and SCL-1 cells by RNAi. After 24 hours, the cells were analyzed for the expression of CHK1 protein. In both cancer cell lines, the CHK1 protein level was reduced in response to AhR inhibition (Figure 39), suggesting that CHK1 may be involved in the AhR-dependent enhancement of apoptosis susceptibility of the SCC cells.

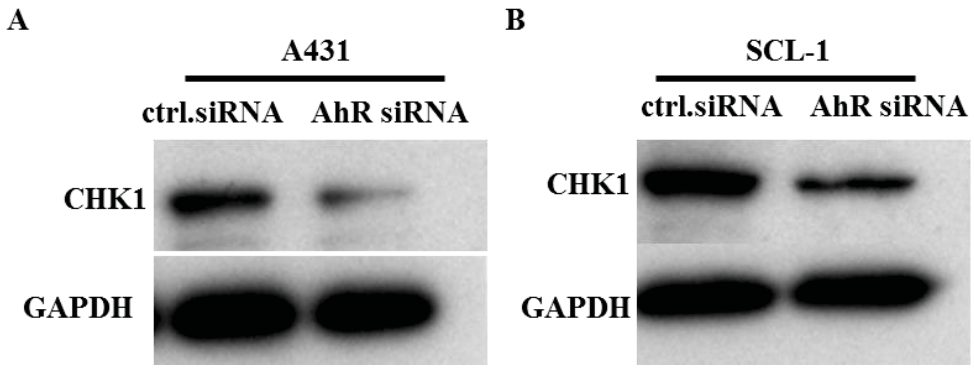

Figure 39 CHK1 expressions in A431 and SCL-1 after AhR inhibition.
A431 and SCL-1 cells were transiently silenced for AhR by the siRNA-mediated knockdown. After 24h western blot analysis was done for CHKI. (A) Expression of CHK1 in A431 cells with and without siRNA-mediated transient AhR knockdown. (B) Expression of CHK1 in SCL-1 cells with and without siRNA-mediated transient AhR knockdown. n=1.

In summary, these results for the first time demonstrate that AhR inhibition influences DNA repair and stimulates apoptosis. Interestingly, in the context of DNA repair, AhR inhibition was shown to promote both CPD clearance and DNA double-strand breaks, indicating that AhR has a dual function in the context of DNA damage.

4. Discussion

NMSC is the most frequently diagnosed cancer in humans. Due to depletion of the ozone layer, an increase in the practice of recreational sunbathing, chronic exposure to UVB radiation, and an increase in the aging population, incidence of NMSC is expected to increase. In elderly people, the skin may have accumulated the damage (Eisemann et al. 2014) due to sun exposure over many years. Therefore, new strategies for modulating DNA damage responses are of tremendous importance for the chemoprevention of UVB-induced skin cancer.

4.1. Importance of CPDs for photo-carcinogenesis

In this work, the molecular function of the AhR in cutaneous UV stress responses, particularly with regard to CPD removal, has been investigated. Irradiation of HaCaT cells with UVB and subsequent treatment with MNF revealed improved CPD clearance. Upon UVB irradiation, CPDs and 6-4 PPs are generated in the DNA. Among these two, CPDs are considered necessary for photo-carcinogenesis. The NER mechanism repairs the CPDs; the un-repaired CPDs may give rise to double-strand breaks and lead to apoptosis. Previously, proinflammatory cytokines such as IL-12 and IL-18 have been shown to be involved in the regulation of the NER machinery by regulating the expression of NER enzymes (Schwarz et al. 2002, Schwarz et al. 2006). The tumour-suppressor gene p53 is known to be involved in the regulation of the DNA repair pathway NER through the upregulation of the expression of damage-specific DNA-binding protein 2 (DDB2) (Hwang et al. 1999). The p53 gene targets cell-cycle arrest in the G1 phase and initiates DNA repair (Hollstein et al. 1991); this is a critical step in cancer formation. If the repair fails, p53 stimulates an increase in the expression of *Bax* and induces apoptosis (Miyashita et al. 1994). Nevertheless, if the p53 gene is mutated, cells with DNA damage continue to proliferate (Koljonen et al. 2006); uncontrolled division of these damaged cells may give rise to cancer (Surget et al. 2013). We observed an improvement in CPD removal in HaCaT cells by chemical or sh-RNA-mediated AhR inhibition. This CPD removal takes place by regulating the GGR subpathway of NER because the MNF-mediated beneficial effect on CPD removal was not abolished after a siRNA-mediated transient silence of CSB (a protein involved in TCR pathway). HaCaT cells are known to have p53 mutations (Boukamp et al. 1988, Lehman et al. 1993). The HaCaT cells may give rise to aberrant p53 responses due to known mutations. This suggests that our results are showing disturbed p53 regulation. This, in turn, points to the idea that p53 may not have been involved in the AhR-dependent GGR in HaCaT cells.

4.2. Influence of AhR on NER

NER is an important excision repair mechanism that removes DNA damage induced by UV-irradiation. It is further divided into two subtypes: GGR and TCR. In the context of skin carcinogenesis, GGR is more important than TCR (Berg et al. 2000). This can be explained by looking at XP and CS patients. XP patients have a deficiency of GGR and CS patients have a deficiency of TCR. TCR repairs the DNA lesions in actively transcribed genes, while GGR repairs the DNA lesions in the whole genome. Hence, in CS patients, if the DNA lesions are not repaired by TCR, GGR probably removes the lesions during DNA replication. Therefore, XP patients are more sensitive to UVB-irradiated skin carcinogenesis (Reid-Bayliss et al. 2016). Since AhR inhibition improves CPD removal faster by regulating the GGR, AhR inhibition can be used as a tool in the prevention of skin carcinogenesis by UVB-irradiation.

Previously, it was shown that UVB-activated AhR stimulates c-Src activity, EGFR, and downstream MAPK pathway to phosphorylate ERK (Fritsche et al. 2007). The western blot results of ERK1/2 inhibition and improved CPD removal from our inhibitor experiments for this cascade suggests that AhR may regulate GGR via the non-canonical AhR pathway. It has been shown that sh-RNA-mediated AhR inhibition leads to enhanced expression of $p27^{KIP1}$ in NCTC cells (Frauenstein et al. 2013). Similarly, in HaCaT cells, MNF-mediated AhR inhibition resulted in enhanced $p27^{KIP1}$, while BaP-mediated AhR-induction led to inhibition of $p27^{KIP1}$ protein levels (Pollet 2015). In a clinical study on colorectal cancer, treatment with EGFR-inhibitor cetuximab resulted in the inhibition of phosphorylation of EGFR and MAPK and increased expression of CDK-inhibitor $p27^{KIP1}$ (Tabernero et al. 2010), indicating a connection between EGFR, MAPK, and $p27^{KIP1}$ in the pathogenesis of cancer.

Overexpression of AhRR resulted in improved CPD removal. Although it is well-established that AhRR inhibits XRE-dependent transcription of AhR by competing with ARNT (Mimura et al. 1999, Haarmann-Stemmann et al. 2007), a low nuclear accumulation and DNA-binding pattern of CCAAT/enhancer binding protein (C/EBP) and NF-kB have been observed in TCDD-exposed transgenic mice (Vogel et al. 2016), suggesting that AhRR may not strictly act in an XRE-dependent manner. Thus, overexpression of AhRR may enhance GGR, However, further mechanistic studies must be performed to strengthen this notion.

The tumour-suppressor protein and CDK-inhibitor $p27^{KIP1}$ is essential for maintaining genome integrity (Chu et al. 2008). Upon DNA damage by ionizing radiation, $p27^{KIP1}$ is critical for stalling the cell in G1 phase and promoting DNA repair (Cassimere et al. 2016). In tumor suppression, $p27^{KIP1}$ is haploinsufficient in murine as well as human leukemia (Fero et al. 1998, Le Toriellec et al. 2008), indicating that low levels of $p27^{KIP1}$ correlate with cancer-proneness. It was demonstrated that oncogenic signal transduction pathways (e.g., AKT) inhibit $p27^{KIP1}$ in various cancers, such as breast cancer (Clarke 2003). In BALB/c 3T3 cells, higher levels of $p27^{KIP1}$ protein were observed in quiescent cells in comparison to the proliferating cells (Agrawal et al. 1995). In addition, it was shown that fully differentiated or non-proliferating primary murine KC express high levels of $p27^{KIP1}$ protein (Hauser et al. 1997). In this context, the results from CPD measurement of non-proliferating HaCaT cells did not support the beneficial effect of AhR inhibition on CPD removal. Treatment with CDK inhibitor, roscovitine after UVB-irradiation led to improved CPD removal, suggesting that CPD removal is cell-cycle-dependent. Transient silencing of $p27^{KIP1}$ in HaCaT cells abolished the MNF-mediated improved CPD clearance and overexpression of $p27^{KIP1}$ promoted improved CPD removal after UVB-irradiation. It has been shown that sh-RNA-mediated AhR inhibition leads to enhanced protein level of $p27^{KIP1}$ in NCTC-sh AhR KC (Frauenstein et al. 2013), indicating that AhR may inhibit NER by targeting proteasomal degradation of $p27^{KIP1}$. Since GGR is cell-cycle-dependent (Demetriou et al. 2012), more experiments are required to explain whether AhR regulates GGR by modulating $p27^{KIP1}$. For instance, cell-cycle analysis experiments can be combined with AhR inhibition of synchronized cells after UVB-irradiation.

Acute and chronic exposure to UVB radiation can lead to local as well as systemic suppression of immune responses, for instance the activation of effector T cells. The major trigger for UVB-induced immunosuppression are CPDs (Stege et al. 2000). It was shown that AhR is involved in the UVR-induced immunosuppression through the modulation of dendritic cells or antigen-specific regulatory T cells, independent of DNA damage in the murine models (Elmets and Athar 2013). Following our results, it may be hypothesized that AhR's modulation of UVB-induced CPD removal may be dependent on immunosuppression. In addition, UVR-activated AhR was shown to represses immune system in a murine model by inducing regulatory T cells in a DNA-damage-independent manner (Navid et al. 2013, Bruhs et al. 2015). However, given the complexity of the immune system, the role of AhR in UV-induced immunosuppression needs to be characterized in depth in appropriate animal models.

4.3. Influence of AhR on UVB-induced apoptosis

Enhanced NER activity should be associated with less apoptosis (Katiyar et al. 2011), surprisingly, we have observed opposite effect, i.e. chemical or sh-RNA-mediated AhR inhibition promoted apoptosis. Apoptosis plays a major role in regulating the development and progression of carcinogenesis. An increased induction of UVB-induced apoptosis could, therefore, have a positive influence in the prevention and treatment of NMSC. In this context, the role of AhR in UVB-induced apoptosis in HaCaT cells should be elucidated. In literature, the influence of the AhR on apoptosis is debated quite controversially. Thus, on the one hand, an increase in apoptosis rate after TGF-β stimulation was observed in the hepatocytes of AhR-deficient mice (Zaher et al. 1998). On the other hand, a pro-apoptotic role of AhR was described in Fas-mediated programmed cell death in hepatocytes (Park et al. 2005). It was shown that low levels of CHK1, associated with AhR inhibition, sensitize cells to apoptosis (Frauenstein et al. 2013). CHKI is essential for arresting the cell-cycle after DNA damage and is a key regulator for maintaining genome integrity through initiating homologous recombinant repair (HRR) (Sorensen et al. 2005). When the unrepaired CPDs are inherent on the template strand during replication, at collapse of the fork at the damaged site may occur, leading to double-strand breaks (Ikehata and Ono 2011). In HeLa cells, concurrent treatment of ruthenium poly pyridyl intercalator and CHK1 inhibitor synergistically increased the apoptosis by inducing double-strand breaks (Gill et al. 2016). The observed increase in double-strand breaks after 18 hours could be due to the loss of CHK1 expression and associated defects in HRR caused by AhR inhibition. However, more experiments should be conducted to confirm a role of AhR and CHK1 in the cellular response to DNA double-strand breaks. For instance, ectopic overexpression of CHK1 should rescue cells from double-strand breaks after AhR inhibition.

AhR plays a critical role in the carcinogenesis of liver, breast and brain cancers (Murray et al. 2014, Go et al. 2015). Apart from its role in the pathophysiology of extracutaneous cancers, the AhR has a major impact on chemical skin carcinogenesis. TCDD promotes dimethyl butylamine (DMBA)-induced skin carcinogenesis in rodents through the sustained activation of AhR (Poland et al. 1982). In addition, AhR-deficient mice were largely protected against PAH-induced skin carcinogenicity (Shimizu et al. 2000, Nakatsuru et al. 2004). With regards to photo-carcinogenesis, AhR activation elevates COX-2, which is critically involved in skin tumorigenesis of SCCs and BCCs (Elmets et al. 2010). Apoptosis is also important during tumor promotion, i.e., the clonal expansion of the initiated cells (Evan and Vousden 2001). Chemical or genetic AhR inhibition sensitized SCC cells to apoptosis, supporting the idea that AhR

inhibitors can be used in the treatment of skin cancer along with other genotoxic cytostatics, such as cisplatin or etoposide. We propose that (topical) AhR antagonism may represent a suitable tool to enhance the efficiency of genotoxic drugs during skin cancer therapy.

In summary, this study demonstrates that AhR inhibition improves CPD removal in UVB-irradiated KC, indicating that AhR antagonism protects against photocarcinogenesis. However, AhR inhibition does not rescue damaged KC from apoptosis, which is probably due to an increased formation of cytotoxic DNA double-strand breaks. Whereas the suitability of AhR antagonists for chemoprevention of UV-induced skin cancer remains to be further investigated, these compounds may be beneficial to increase the efficiency of genotoxic anti-cancer drugs.

References

Abel, J., and T. Haarmann-Stemmann. 2010. An introduction to the molecular basics of aryl hydrocarbon receptor biology. Biol Chem **391**:1235-1248.

Agostinis, P., M. Garmyn, and A. Van Laethem. 2007. The Aryl hydrocarbon receptor: an illuminating effector of the UVB response. Sci STKE **2007**:pe49.

Agrawal, D., F. Dong, Y. Z. Wang, D. Kayda, and W. J. Pledger. 1995. Regulation of cyclin E and p27kip during mitosis in BALB/c 3T3 cells. Cell Growth Differ **6**:1199-1205.

Barolet, D., F. Christiaens, and M. R. Hamblin. 2016. Infrared and skin: Friend or foe. J Photochem Photobiol B **155**:78-85.

Baroni, A., E. Buommino, V. De Gregorio, E. Ruocco, V. Ruocco, and R. Wolf. 2012. Structure and function of the epidermis related to barrier properties. Clin Dermatol **30**:257-262.

Berg, R. J., H. Rebel, G. T. van der Horst, H. J. van Kranen, L. H. Mullenders, W. A. van Vloten, and F. R. de Gruijl. 2000. Impact of global genome repair versus transcription-coupled repair on ultraviolet carcinogenesis in hairless mice. Cancer Res **60**:2858-2863.

Berneburg, M., and J. Krutmann. 2000. Photoimmunology, DNA repair and photocarcinogenesis. J Photochem Photobiol B **54**:87-93.

Bock, K. W., and C. Kohle. 2009. The mammalian aryl hydrocarbon (Ah) receptor: from mediator of dioxin toxicity toward physiological functions in skin and liver. Biol Chem **390**:1225-1235.

Bothe, H., C. Gotz, N. Stobbe-Maicherski, E. Fritsche, J. Abel, and T. Haarmann-Stemmann. 2010. Luteolin enhances the bioavailability of benzo(a)pyrene in human colon carcinoma cells. Arch Biochem Biophys **498**:111-118.

Boukamp, P., R. T. Petrussevska, D. Breitkreutz, J. Hornung, A. Markham, and N. E. Fusenig. 1988. Normal keratinization in a spontaneously immortalized aneuploid human keratinocyte cell line. J Cell Biol **106**:761-771.

Boukamp, P., W. Tilgen, R. T. Dzarlieva, D. Breitkreutz, D. Haag, R. K. Riehl, A. Bohnert, and N. E. Fusenig. 1982. Phenotypic and genotypic characteristics of a cell line from a squamous cell carcinoma of human skin. J Natl Cancer Inst **68**:415-427.

Bowden, G. T. 2004. Prevention of non-melanoma skin cancer by targeting ultraviolet-B-light signalling. Nat Rev Cancer **4**:23-35.

Brash, D. E. 1988. UV mutagenic photoproducts in Escherichia coli and human cells: a molecular genetics perspective on human skin cancer. Photochem Photobiol **48**:59-66.

Brash, D. E., and J. Ponten. 1998. Skin precancer. Cancer Surv **32**:69-113.

Bratton, D. L., V. A. Fadok, D. A. Richter, J. M. Kailey, L. A. Guthrie, and P. M. Henson. 1997. Appearance of phosphatidylserine on apoptotic cells requires calcium-mediated nonspecific flip-flop and is enhanced by loss of the aminophospholipid translocase. J Biol Chem **272**:26159-26165.

Bruhs, A., T. Haarmann-Stemmann, K. Frauenstein, J. Krutmann, T. Schwarz, and A. Schwarz. 2015. Activation of the arylhydrocarbon receptor causes immunosuppression primarily by modulating dendritic cells. J Invest Dermatol **135**:435-444.

Bukowsky, L. F. 2010. Skin anatomy and physiology research developments. Nova science publisher.

Cassimere, E. K., C. Mauvais, and C. Denicourt. 2016. p27Kip1 Is Required to Mediate a G1 Cell Cycle Arrest Downstream of ATM following Genotoxic Stress. PLoS One **11**:e0162806.

Chen, P. H., H. Chang, J. T. Chang, and P. Lin. 2012. Aryl hydrocarbon receptor in association with RelA modulates IL-6 expression in non-smoking lung cancer. Oncogene **31**:2555-2565.

Chigancas, V., L. F. Batista, G. Brumatti, G. P. Amarante-Mendes, A. Yasui, and C. F. Menck. 2002. Photorepair of RNA polymerase arrest and apoptosis after ultraviolet irradiation in normal and XPB deficient rodent cells. Cell Death Differ **9**:1099-1107.

Chu, I. M., L. Hengst, and J. M. Slingerland. 2008. The Cdk inhibitor p27 in human cancer: prognostic potential and relevance to anticancer therapy. Nat Rev Cancer **8**:253-267.

Ciolino, H. P., P. J. Daschner, T. T. Wang, and G. C. Yeh. 1998. Effect of curcumin on the aryl hydrocarbon receptor and cytochrome P450 1A1 in MCF-7 human breast carcinoma cells. Biochem Pharmacol **56**:197-206.

Ciolino, H. P., P. J. Daschner, and G. C. Yeh. 1999. Dietary flavonols quercetin and kaempferol are ligands of the aryl hydrocarbon receptor that affect CYP1A1 transcription differentially. Biochem J **340 (Pt 3)**:715-722.

Ciolino, H. P., and G. C. Yeh. 1999. Inhibition of aryl hydrocarbon-induced cytochrome P-450 1A1 enzyme activity and CYP1A1 expression by resveratrol. Mol Pharmacol **56**:760-767.

Citri, Y., H. V. Colot, A. C. Jacquier, Q. Yu, J. C. Hall, D. Baltimore, and M. Rosbash. 1987. A family of unusually spliced biologically active transcripts encoded by a Drosophila clock gene. Nature **326**:42-47.

Clarke, R. B. 2003. p27KIP1 phosphorylation by PKB/Akt leads to poor breast cancer prognosis. Breast Cancer Res **5**:162-163.

Coin, F., J. Auriol, A. Tapias, P. Clivio, W. Vermeulen, and J. M. Egly. 2004. Phosphorylation of XPB helicase regulates TFIIH nucleotide excision repair activity. Embo j **23**:4835-4846.

Delescluse, C., N. Ledirac, R. Li, M. P. Piechocki, R. N. Hines, X. Gidrol, and R. Rahmani. 2001. Induction of cytochrome P450 1A1 gene expression, oxidative stress, and genotoxicity by carbaryl and thiabendazole in transfected human HepG2 and lymphoblastoid cells. Biochem Pharmacol **61**:399-407.

Demetriou, S. K., K. Ona-Vu, E. M. Sullivan, T. K. Dong, S. W. Hsu, and D. H. Oh. 2012. Defective DNA repair and cell cycle arrest in cells expressing Merkel cell polyomavirus T antigen. Int J Cancer **131**:1818-1827.

Denis, M., S. Cuthill, A. C. Wikstrom, L. Poellinger, and J. A. Gustafsson. 1988. Association of the dioxin receptor with the Mr 90,000 heat shock protein: a structural kinship with the glucocorticoid receptor. Biochem Biophys Res Commun **155**:801-807.

Denison, M. S., and S. R. Nagy. 2003. Activation of the aryl hydrocarbon receptor by structurally diverse exogenous and endogenous chemicals. Annu Rev Pharmacol Toxicol **43**:309-334.

Eisemann, N., A. Waldmann, A. C. Geller, M. A. Weinstock, B. Volkmer, R. Greinert, E. W. Breitbart, and A. Katalinic. 2014. Non-melanoma skin cancer incidence and impact of skin cancer screening on incidence. J Invest Dermatol **134**:43-50.

El-Mahdy, M. A., Q. Zhu, Q. E. Wang, G. Wani, S. Patnaik, Q. Zhao, S. Arafa el, B. Barakat, S. N. Mir, and A. A. Wani. 2008. Naringenin protects HaCaT human keratinocytes against UVB-induced apoptosis and enhances the removal of cyclobutane pyrimidine dimers from the genome. Photochem Photobiol **84**:307-316.

Elmets, C. A., and M. Athar. 2013. Milestones in photocarcinogenesis. J Invest Dermatol **133**:E13-17.

Elmets, C. A., J. L. Viner, A. P. Pentland, W. Cantrell, H. Y. Lin, H. Bailey, S. Kang, K. G. Linden, M. Heffernan, M. Duvic, E. Richmond, B. E. Elewski, A. Umar, W. Bell, and G. B. Gordon. 2010. Chemoprevention of nonmelanoma skin cancer with celecoxib: a randomized, double-blind, placebo-controlled trial. J Natl Cancer Inst **102**:1835-1844.

Enan, E., and F. Matsumura. 1996. Identification of c-Src as the integral component of the cytosolic Ah receptor complex, transducing the signal of 2,3,7,8-tetrachlorodibenzo-p-

dioxin (TCDD) through the protein phosphorylation pathway. Biochem Pharmacol **52**:1599-1612.

Evan, G. I., and K. H. Vousden. 2001. Proliferation, cell cycle and apoptosis in cancer. Nature **411**:342-348.

Farmahin, R., D. Crump, and S. W. Kennedy. 2014. Sensitivity of avian species to the aryl hydrocarbon receptor ligand 6-formylindolo [3,2-b] carbazole (FICZ). Chem Biol Interact **221**:61-69.

Fero, M. L., E. Randel, K. E. Gurley, J. M. Roberts, and C. J. Kemp. 1998. The murine gene p27Kip1 is haplo-insufficient for tumour suppression. Nature **396**:177-180.

Frauenstein, K., U. Sydlik, J. Tigges, M. Majora, C. Wiek, H. Hanenberg, J. Abel, C. Esser, E. Fritsche, J. Krutmann, and T. Haarmann-Stemmann. 2013. Evidence for a novel anti-apoptotic pathway in human keratinocytes involving the aryl hydrocarbon receptor, E2F1, and checkpoint kinase 1. Cell Death Differ **20**:1425-1434.

Fritsche, E., C. Schafer, C. Calles, T. Bernsmann, T. Bernshausen, M. Wurm, U. Hubenthal, J. E. Cline, H. Hajimiragha, P. Schroeder, L. O. Klotz, A. Rannug, P. Furst, H. Hanenberg, J. Abel, and J. Krutmann. 2007. Lightening up the UV response by identification of the arylhydrocarbon receptor as a cytoplasmatic target for ultraviolet B radiation. Proc Natl Acad Sci U S A **104**:8851-8856.

Ghantous, A., M. Saikali, T. Rau, H. Gali-Muhtasib, R. Schneider-Stock, and N. Darwiche. 2012. Inhibition of tumor promotion by parthenolide: epigenetic modulation of p21. Cancer Prev Res (Phila) **5**:1298-1309.

Giard, D. J., S. A. Aaronson, G. J. Todaro, P. Arnstein, J. H. Kersey, H. Dosik, and W. P. Parks. 1973. In vitro cultivation of human tumors: establishment of cell lines derived from a series of solid tumors. J Natl Cancer Inst **51**:1417-1423.

Gill, M. R., S. N. Harun, S. Halder, R. A. Boghozian, K. Ramadan, H. Ahmad, and K. A. Vallis. 2016. A ruthenium polypyridyl intercalator stalls DNA replication forks, radiosensitizes human cancer cells and is enhanced by Chk1 inhibition. Sci Rep **6**:31973.

Go, R. E., K. A. Hwang, and K. C. Choi. 2015. Cytochrome P450 1 family and cancers. J Steroid Biochem Mol Biol **147**:24-30.

Gu, Y. Z., J. B. Hogenesch, and C. A. Bradfield. 2000. The PAS superfamily: sensors of environmental and developmental signals. Annu Rev Pharmacol Toxicol **40**:519-561.

Haarmann-Stemmann, T., J. Abel, E. Fritsche, and J. Krutmann. 2012. The AhR-Nrf2 pathway in keratinocytes: on the road to chemoprevention? J Invest Dermatol **132**:7-9.

Haarmann-Stemmann, T., H. Bothe, and J. Abel. 2009. Growth factors, cytokines and their receptors as downstream targets of arylhydrocarbon receptor (AhR) signaling pathways. Biochem Pharmacol **77**:508-520.

Haarmann-Stemmann, T., H. Bothe, A. Kohli, U. Sydlik, J. Abel, and E. Fritsche. 2007. Analysis of the transcriptional regulation and molecular function of the aryl hydrocarbon receptor repressor in human cell lines. Drug Metab Dispos **35**:2262-2269.

Hauser, P. J., D. Agrawal, M. Flanagan, and W. J. Pledger. 1997. The role of p27kip1 in the in vitro differentiation of murine keratinocytes. Cell Growth Differ **8**:203-211.

Herrlich, P., M. Karin, and C. Weiss. 2008. Supreme EnLIGHTenment: damage recognition and signaling in the mammalian UV response. Mol Cell **29**:279-290.

Hoffman, M. 2014. Picture of the skin, human anatomy. Web MD.

Hollstein, M., D. Sidransky, B. Vogelstein, and C. C. Harris. 1991. p53 mutations in human cancers. Science **253**:49-53.

Hwang, B. J., J. M. Ford, P. C. Hanawalt, and G. Chu. 1999. Expression of the p48 xeroderma pigmentosum gene is p53-dependent and is involved in global genomic repair. Proc Natl Acad Sci U S A **96**:424-428.

Ikehata, H., and T. Ono. 2011. The mechanisms of UV mutagenesis. J Radiat Res **52**:115-125.

Jain, S. 2012. Dermatology Basic Science and Immunology. Springer, Springer New York Dordrecht Heidelberg London.

Katiyar, S. K., S. K. Mantena, and S. M. Meeran. 2011. Silymarin protects epidermal keratinocytes from ultraviolet radiation-induced apoptosis and DNA damage by nucleotide excision repair mechanism. PLoS One **6**:e21410.

Katiyar, S. K., M. S. Matsui, and H. Mukhtar. 2000. Ultraviolet-B exposure of human skin induces cytochromes P450 1A1 and 1B1. J Invest Dermatol **114**:328-333.

Kazlauskas, A., L. Poellinger, and I. Pongratz. 1999. Evidence that the co-chaperone p23 regulates ligand responsiveness of the dioxin (Aryl hydrocarbon) receptor. J Biol Chem **274**:13519-13524.

Koljonen, V., E. Tukiainen, C. Haglund, and T. Bohling. 2006. Cell cycle control by p21, p27 and p53 in Merkel cell carcinoma. Anticancer Res **26**:2209-2212.

Krutmann, J., A. Morita, and J. H. Chung. 2012. Sun exposure: what molecular photodermatology tells us about its good and bad sides. J Invest Dermatol **132**:976-984.

Kubo, A., K. Nagao, M. Yokouchi, H. Sasaki, and M. Amagai. 2009. External antigen uptake by Langerhans cells with reorganization of epidermal tight junction barriers. J Exp Med **206**:2937-2946.

Kulms, D., and T. Schwarz. 2000. Molecular mechanisms of UV-induced apoptosis. Photodermatol Photoimmunol Photomed **16**:195-201.

Kuo, L. J., and L. X. Yang. 2008. Gamma-H2AX - a novel biomarker for DNA double-strand breaks. In Vivo **22**:305-309.

Le Toriellec, E., G. Despouy, G. Pierron, N. Gaye, M. Joiner, D. Bellanger, A. Vincent-Salomon, and M. H. Stern. 2008. Haploinsufficiency of CDKN1B contributes to leukemogenesis in T-cell prolymphocytic leukemia. Blood **111**:2321-2328.

Lehman, T. A., R. Modali, P. Boukamp, J. Stanek, W. P. Bennett, J. A. Welsh, R. A. Metcalf, M. R. Stampfer, N. Fusenig, E. M. Rogan, and et al. 1993. p53 mutations in human immortalized epithelial cell lines. Carcinogenesis **14**:833-839.

Lindahl, T., and R. D. Wood. 1999. Quality control by DNA repair. Science **286**:1897-1905.

Lips, J., and B. Kaina. 2001. DNA double-strand breaks trigger apoptosis in p53-deficient fibroblasts. Carcinogenesis **22**:579-585.

Lu, Y. F., M. Santostefano, B. D. Cunningham, M. D. Threadgill, and S. Safe. 1995. Identification of 3'-methoxy-4'-nitroflavone as a pure aryl hydrocarbon (Ah) receptor antagonist and evidence for more than one form of the nuclear Ah receptor in MCF-7 human breast cancer cells. Arch Biochem Biophys **316**:470-477.

Ma, Q., and J. P. Whitlock, Jr. 1997. A novel cytoplasmic protein that interacts with the Ah receptor, contains tetratricopeptide repeat motifs, and augments the transcriptional response to 2,3,7,8-tetrachlorodibenzo-p-dioxin. J Biol Chem **272**:8878-8884.

Marteijn, J. A., H. Lans, W. Vermeulen, and J. H. Hoeijmakers. 2014. Understanding nucleotide excision repair and its roles in cancer and ageing. Nat Rev Mol Cell Biol **15**:465-481.

Martínez-Lozano, J. A., F. Tena, M. J. Marín, M. P. Utrillas, J. Lorente, X. De Cabo, and C. González-Frías. 2002. Experimental values of the UV index during 2000 at two locations in Mediterranean Spain. International Journal of Climatology **22**:501-508.

Matikainen, T., G. I. Perez, A. Jurisicova, J. K. Pru, J. J. Schlezinger, H. Y. Ryu, J. Laine, T. Sakai, S. J. Korsmeyer, R. F. Casper, D. H. Sherr, and J. L. Tilly. 2001. Aromatic hydrocarbon receptor-driven Bax gene expression is required for premature ovarian failure caused by biohazardous environmental chemicals. Nat Genet **28**:355-360.

Maverakis, E., Y. Miyamura, M. P. Bowen, G. Correa, Y. Ono, and H. Goodarzi. 2010. Light, Including Ultraviolet. Journal of autoimmunity **34**:J247-J257.

Meador, J. A., R. B. Walter, and D. L. Mitchell. 2000. Induction, distribution and repair of UV photodamage in the platyfish, Xiphophorus signum. Photochem Photobiol **72**:260-266.

Meeran, S. M., S. K. Mantena, C. A. Elmets, and S. K. Katiyar. 2006. (-)-Epigallocatechin-3-gallate prevents photocarcinogenesis in mice through interleukin-12-dependent DNA repair. Cancer Res **66**:5512-5520.

Mimura, J., M. Ema, K. Sogawa, and Y. Fujii-Kuriyama. 1999. Identification of a novel mechanism of regulation of Ah (dioxin) receptor function. Genes Dev **13**:20-25.

Miyamura, Y., S. G. Coelho, R. Wolber, S. A. Miller, K. Wakamatsu, B. Z. Zmudzka, S. Ito, C. Smuda, T. Passeron, W. Choi, J. Batzer, Y. Yamaguchi, J. Z. Beer, and V. J. Hearing. 2007. Regulation of human skin pigmentation and responses to ultraviolet radiation. Pigment Cell Res **20**:2-13.

Miyashita, T., S. Krajewski, M. Krajewska, H. G. Wang, H. K. Lin, D. A. Liebermann, B. Hoffman, and J. C. Reed. 1994. Tumor suppressor p53 is a regulator of bcl-2 and bax gene expression in vitro and in vivo. Oncogene **9**:1799-1805.

Moll, I., M. Roessler, J. M. Brandner, A. C. Eispert, P. Houdek, and R. Moll. 2005. Human Merkel cells--aspects of cell biology, distribution and functions. Eur J Cell Biol **84**:259-271.

Murray, I. A., A. D. Patterson, and G. H. Perdew. 2014. Aryl hydrocarbon receptor ligands in cancer: friend and foe. Nat Rev Cancer **14**:801-814.

Nakatsuru, Y., K. Wakabayashi, Y. Fujii-Kuriyama, T. Ishikawa, K. Kusama, and F. Ide. 2004. Dibenzo[A,L]pyrene-induced genotoxic and carcinogenic responses are dramatically suppressed in aryl hydrocarbon receptor-deficient mice. Int J Cancer **112**:179-183.

Nambu, J. R., J. O. Lewis, K. A. Wharton, Jr., and S. T. Crews. 1991. The Drosophila single-minded gene encodes a helix-loop-helix protein that acts as a master regulator of CNS midline development. Cell **67**:1157-1167.

Navid, F., A. Bruhs, W. Schuller, E. Fritsche, J. Krutmann, T. Schwarz, and A. Schwarz. 2013. The Aryl hydrocarbon receptor is involved in UVR-induced immunosuppression. J Invest Dermatol **133**:2763-2770.

Olive, P. L., G. Frazer, and J. P. Banath. 1993. Radiation-induced apoptosis measured in TK6 human B lymphoblast cells using the comet assay. Radiat Res **136**:130-136.

Palermo, C. M., J. I. Hernando, S. D. Dertinger, A. S. Kende, and T. A. Gasiewicz. 2003. Identification of potential aryl hydrocarbon receptor antagonists in green tea. Chem Res Toxicol **16**:865-872.

Park, K. T., K. A. Mitchell, G. Huang, and C. J. Elferink. 2005. The aryl hydrocarbon receptor predisposes hepatocytes to Fas-mediated apoptosis. Mol Pharmacol **67**:612-622.

Pentland, A. P., J. W. Schoggins, G. A. Scott, K. N. Khan, and R. Han. 1999. Reduction of UV-induced skin tumors in hairless mice by selective COX-2 inhibition. Carcinogenesis **20**:1939-1944.

Poland, A., D. Palen, and E. Glover. 1982. Tumour promotion by TCDD in skin of HRS/J hairless mice. Nature **300**:271-273.

Pollet, M. 2015. Untersuchungen zur zellspezifischen Regulation des Tumorsuppressors $p27^{KIP1}$ durch den Arylhydrocarbon Rezeptor. Master thesis. HHU.

Probst, M. R., S. Reisz-Porszasz, R. V. Agbunag, M. S. Ong, and O. Hankinson. 1993. Role of the aryl hydrocarbon receptor nuclear translocator protein in aryl hydrocarbon (dioxin) receptor action. Mol Pharmacol **44**:511-518.

Puntarulo, S., and A. I. Cederbaum. 1998. Production of reactive oxygen species by microsomes enriched in specific human cytochrome P450 enzymes. Free Radic Biol Med **24**:1324-1330.

Qin, X., S. Zhang, Y. Nakatsuru, H. Oda, Y. Yamazaki, T. Suzuki, O. Nikaido, and T. Ishikawa. 1994. Detection of active UV-photoproduct repair in monkey skin in vivo by quantitative immunohistochemistry. Cancer Lett **83**:291-298.

Quattrochi, L. C., and R. H. Tukey. 1993. Nuclear uptake of the Ah (dioxin) receptor in response to omeprazole: transcriptional activation of the human CYP1A1 gene. Mol Pharmacol **43**:504-508.

Rakoff-Nahoum, S. 2006. Why cancer and inflammation? Yale J Biol Med **79**:123-130.

Rannug, A., U. Rannug, H. S. Rosenkranz, L. Winqvist, R. Westerholm, E. Agurell, and A. K. Grafstrom. 1987. Certain photooxidized derivatives of tryptophan bind with very high affinity to the Ah receptor and are likely to be endogenous signal substances. J Biol Chem **262**:15422-15427.

Reid-Bayliss, K. S., S. T. Arron, L. A. Loeb, V. Bezrookove, and J. E. Cleaver. 2016. Why Cockayne syndrome patients do not get cancer despite their DNA repair deficiency. Proc Natl Acad Sci U S A **113**:10151-10156.

Robinson, J. K. 2005. Sun exposure, sun protection, and vitamin D. Jama **294**:1541-1543.

Rowlands, J. C., I. J. McEwan, and J. A. Gustafsson. 1996. Trans-activation by the human aryl hydrocarbon receptor and aryl hydrocarbon receptor nuclear translocator proteins: direct interactions with basal transcription factors. Mol Pharmacol **50**:538-548.

Schroeder, P., C. Calles, and J. Krutmann. 2009. Prevention of infrared-A radiation mediated detrimental effects in human skin. Skin Therapy Lett **14**:4-5.

Schroeder, P., J. Haendeler, and J. Krutmann. 2008a. The role of near infrared radiation in photoaging of the skin. Exp Gerontol **43**:629-632.

Schroeder, P., J. Lademann, M. E. Darvin, H. Stege, C. Marks, S. Bruhnke, and J. Krutmann. 2008b. Infrared radiation-induced matrix metalloproteinase in human skin: implications for protection. J Invest Dermatol **128**:2491-2497.

Schwarz, A., A. Maeda, S. Stander, H. van Steeg, and T. Schwarz. 2006. IL-18 reduces ultraviolet radiation-induced DNA damage and thereby affects photoimmunosuppression. J Immunol **176**:2896-2901.

Schwarz, A., S. Stander, M. Berneburg, M. Bohm, D. Kulms, H. van Steeg, K. Grosse-Heitmeyer, J. Krutmann, and T. Schwarz. 2002. Interleukin-12 suppresses ultraviolet radiation-induced apoptosis by inducing DNA repair. Nat Cell Biol **4**:26-31.

Shimizu, Y., Y. Nakatsuru, M. Ichinose, Y. Takahashi, H. Kume, J. Mimura, Y. Fujii-Kuriyama, and T. Ishikawa. 2000. Benzo[a]pyrene carcinogenicity is lost in mice lacking the aryl hydrocarbon receptor. Proc Natl Acad Sci U S A **97**:779-782.

Sklar, L. R., F. Almutawa, H. W. Lim, and I. Hamzavi. 2013. Effects of ultraviolet radiation, visible light, and infrared radiation on erythema and pigmentation: a review. Photochem Photobiol Sci **12**:54-64.

Song, J., M. Clagett-Dame, R. E. Peterson, M. E. Hahn, W. M. Westler, R. R. Sicinski, and H. F. DeLuca. 2002. A ligand for the aryl hydrocarbon receptor isolated from lung. Proc Natl Acad Sci U S A **99**:14694-14699.

Sorensen, C. S., L. T. Hansen, J. Dziegielewski, R. G. Syljuasen, C. Lundin, J. Bartek, and T. Helleday. 2005. The cell-cycle checkpoint kinase Chk1 is required for mammalian homologous recombination repair. Nat Cell Biol **7**:195-201.

Stege, H., L. Roza, A. A. Vink, M. Grewe, T. Ruzicka, S. Grether-Beck, and J. Krutmann. 2000. Enzyme plus light therapy to repair DNA damage in ultraviolet-B-irradiated human skin. Proc Natl Acad Sci U S A **97**:1790-1795.

Surget, S., M. P. Khoury, and J. C. Bourdon. 2013. Uncovering the role of p53 splice variants in human malignancy: a clinical perspective. Onco Targets Ther **7**:57-68.

Tabernero, J., A. Cervantes, F. Rivera, E. Martinelli, F. Rojo, A. von Heydebreck, T. Macarulla, E. Rodriguez-Braun, M. Eugenia Vega-Villegas, S. Senger, F. J. Ramos, S. Rosello, I. Celik, C. Stroh, J. Baselga, and F. Ciardiello. 2010. Pharmacogenomic and pharmacoproteomic studies of cetuximab in metastatic colorectal cancer: biomarker analysis of a phase I dose-escalation study. J Clin Oncol **28**:1181-1189.

Tian, Y. 2009. Ah receptor and NF-kappaB interplay on the stage of epigenome. Biochem Pharmacol **77**:670-680.

Vanden Heuvel, J. P., G. C. Clark, C. L. Thompson, Z. McCoy, C. R. Miller, G. W. Lucier, and D. A. Bell. 1993. CYP1A1 mRNA levels as a human exposure biomarker: use of quantitative polymerase chain reaction to measure CYP1A1 expression in human peripheral blood lymphocytes. Carcinogenesis **14**:2003-2006.

Vogel, C. F., W. L. Chang, S. Kado, K. McCulloh, H. Vogel, D. Wu, T. Haarmann-Stemmann, G. Yang, P. S. Leung, F. Matsumura, and M. E. Gershwin. 2016. Transgenic Overexpression of Aryl Hydrocarbon Receptor Repressor (AhRR) and AhR-Mediated Induction of CYP1A1, Cytokines, and Acute Toxicity. Environ Health Perspect **124**:1071-1083.

Vogel, C. F., W. Li, D. Wu, J. K. Miller, C. Sweeney, G. Lazennec, Y. Fujisawa, and F. Matsumura. 2011. Interaction of aryl hydrocarbon receptor and NF-kappaB subunit RelB in breast cancer is associated with interleukin-8 overexpression. Arch Biochem Biophys **512**:78-86.

Vogel, C. F., E. Sciullo, and F. Matsumura. 2007. Involvement of RelB in aryl hydrocarbon receptor-mediated induction of chemokines. Biochem Biophys Res Commun **363**:722-726.

Wei, Y. D., H. Helleberg, U. Rannug, and A. Rannug. 1998. Rapid and transient induction of CYP1A1 gene expression in human cells by the tryptophan photoproduct 6-formylindolo[3,2-b]carbazole. Chem Biol Interact **110**:39-55.

WHO. Skin cancers. Ultraviolet radiation and the intersun programme. World Health Organization.

WHO. 2012. RADIATION. WHO International Agency for Research on cancer, LYON FRANCE.

Wincent, E., N. Amini, S. Luecke, H. Glatt, J. Bergman, C. Crescenzi, A. Rannug, and U. Rannug. 2009. The suggested physiologic aryl hydrocarbon receptor activator and cytochrome P4501 substrate 6-formylindolo[3,2-b]carbazole is present in humans. J Biol Chem **284**:2690-2696.

Wood, R. D. 1999. DNA repair. Variants on a theme. Nature **399**:639-640.

Yarosh, D., L. G. Alas, V. Yee, A. Oberyszyn, J. T. Kibitel, D. Mitchell, R. Rosenstein, A. Spinowitz, and M. Citron. 1992. Pyrimidine dimer removal enhanced by DNA repair liposomes reduces the incidence of UV skin cancer in mice. Cancer Res **52**:4227-4231.

Zaher, H., P. M. Fernandez-Salguero, J. Letterio, M. S. Sheikh, A. J. Fornace, Jr., A. B. Roberts, and F. J. Gonzalez. 1998. The involvement of aryl hydrocarbon receptor in the activation of transforming growth factor-beta and apoptosis. Mol Pharmacol **54**:313-321.

Zhang, S., C. Qin, and S. H. Safe. 2003. Flavonoids as aryl hydrocarbon receptor agonists/antagonists: effects of structure and cell context. Environ Health Perspect **111**:1877-1882.

Acknowledgements

I would like to express my gratitude to everyone who made it possible for me to complete this thesis. I am especially thankful for:
Professor Jean Krutmann for being my supervisor and granting me the unique opportunity to work in your team at IUF. You have been an excellent supervisor. Thank you for your careful guidance, and warm encouragement. Furthermore, I would like to thank professor Peter Proksch for being my co-supervisor.

I would like to thank Dr. Thomas Haarmann-Stemmann for all his support in my social and scientific life especially; you have been a role model to me.

I am also thankful to my colleagues:
Thanks to Marius Pollet for being supportive all the time and fruitful discussions. Motoki Nakamura, you have been my best friend, and I enjoy all the weekend trips we did together. Melina Meshar thanks for your friendly, supportiveness and no worries attitude. Eli, you have been a part of my family with all the great suggestions both scientifically and socially. Philipp Worst you have been my great friend, and you were always helping me with the German documents and visa processing. Katrin Frauenstein thank you for introducing me the lab techniques and guiding me with all the beginning experiments and being a good friend. Kerstin Fischer and Birgit Neumann thanks for helping me with western blots and PCR. Ragnhild Wirth thank you for your company and advice in western blotting. Katharina Rolfes, you were also my nice friend and I cannot forget the horse rides and visits to horse staple. Mana I would like to thank you for your company and discussions during the coffee breaks. Kevin Sondenheimer thanks for teaching me FACS analysis. Julia Colling thanks a lot for teaching me comet assay. Julia Tigges thank you for answering all my silly questions whenever I asked you. Apart from this, I would like to thank all my colleagues from IUF who have been friendly and supportive to me.

Special thanks to Agneta Rannug for highly recommending me to Dr. Thomas Haarmann-Stemmann. Ulf Rannug for the kind hospitality when we visited you in Italy. Thank you, Maria Jönsson, for being my teacher and best friend. Ingvar Brandt and Björn Brunström, I should thank you for your guidance and motivation to me.

I would like to thank Iftekhar, Saranya, and Anusha for correcting my English and grammar as well as being supportive.

My friends in India and Sweden thanks for all the phone conversations, making my social life joyful.

I would like to thank Rizwana's parents and brothers for being supportive, special thanks to mother-in-law for coming over to Germany and helping us in the early days of my baby.

I would like to thank my parents, sisters, and cousins for being with me in all the stages of my life, for all the support and love they showed me.

Finally, I wish to express my gratitude to my love, Rizwana, for your invaluable support. Thank you, for letting me work late hours without complaints, and for always having good advice, for believing in me, and for being there for me in hard times. Siddiah, my daughter, for filling my life with play, joy, and laughter, you are amazing.

Declaration

I declare under oath that I have compiled my dissertation independently and without any undue assistance by third parties under consideration of the ‘Principles for the Safeguarding of Good Scientific Practice at Heinrich Heine University Düsseldorf.'

This dissertation has not been submitted in its present or a similar form in any other institution. I have not made any successful or unsuccessful attempt to obtain a doctorate before.

Düsseldorf, 21-12.2016

(Siraz Shaik)